

## Dark energy, spatial curvature, and star formation efficiency from JWST photometric and spectroscopic high-redshift galaxies

LEONARDO COMINI <sup>1</sup>, SUNNY VAGNOZZI <sup>1,2</sup> AND ABRAHAM LOEB <sup>3</sup>

<sup>1</sup>*Department of Physics, University of Trento, Via Sommarive 14, 38123 Povo (TN), Italy*

<sup>2</sup>*Trento Institute for Fundamental Physics and Applications (TIFPA)-INFN, Via Sommarive 14, 38123 Povo (TN), Italy*

<sup>3</sup>*Department of Astronomy, Harvard University, 60 Garden Street, Cambridge, MA 02138, USA*

### ABSTRACT

Early observations from the James Webb Space Telescope (JWST) have revealed an overabundance of massive high-redshift galaxies, raising the question of whether this points to new physics beyond  $\Lambda$ CDM, or an enhanced formation efficiency of massive stars. We revisit this issue going beyond earlier analyses based on direct comparisons to theoretical bounds at a fixed cosmology, by performing a full Bayesian analysis of the most extreme galaxies in the CEERS imaging and FRESCO spectroscopic samples, jointly constraining cosmological parameters and the baryon-to-star conversion efficiency  $\epsilon$ . We do so not only within the spatially flat  $\Lambda$ CDM model, but also in models where the dark energy equation of state  $w$  and/or the spatial curvature parameter  $\Omega_K$  are allowed to vary, carefully discussing the impact of both  $w$  and  $\Omega_K$  on the cumulative comoving stellar mass density. Within the flat  $\Lambda$ CDM model, once cosmological parameters are marginalized over, the CEERS sample provides a weak  $2\sigma$  lower limit of  $\epsilon \gtrsim 0.07$ , compatible with astrophysical expectations. In contrast, the FRESCO sample requires  $\epsilon \gtrsim 0.5$  at  $2\sigma$ , with values  $\epsilon \lesssim 0.2$  disfavored at  $> 5\sigma$ . These results do not qualitatively change when we allow  $w$  and/or  $\Omega_K$  to vary, with no evidence for deviations from  $w = -1$  or  $\Omega_K = 0$ . Our results therefore suggest that the origin of the “JWST tension” is unlikely to be cosmological, but lies in the astrophysics of galaxy formation.

*Keywords:* dark energy — cosmology — cosmological parameters — high-redshift galaxies

### 1. INTRODUCTION

The *James Webb Space Telescope* (JWST), a space-based infrared observatory designed to study the formation of the first galaxies and stars (Gardner et al. 2006), is providing a unique view of sources at redshifts up to  $z \sim 15$ , corresponding to the first few hundred million years of cosmic history. This regime, previously only indirectly constrained by low-redshift observations, is one where both the efficiency of early star formation and the growth of structure are still very uncertain. The most massive high-redshift galaxies are particularly interesting in this sense, as they populate the most massive dark matter (DM) halos, whose abundance depends very strongly on the underlying cosmology. Such systems therefore provide a very powerful probe of both cosmology and the physics of galaxy formation.

Early JWST imaging obtained with the Near Infrared Camera (NIRCam) as part of the Cosmic Evolution Early Release Science (CEERS) program led to the identification of a surprisingly high abundance of extremely massive galaxies (with stellar masses exceeding  $\sim 10^{10} M_\odot$ ) at redshifts  $6 \lesssim z \lesssim 10$  (Labbé et al. 2023). As demonstrated by Boylan-Kolchin (2023), the abundance of such systems can be used to stress test cosmological models in a conservative way with minimal assumptions about galaxy formation physics. In particular, considering objects of a given stellar mass, an upper limit on their cumulative comoving stellar mass density can be obtained once the cosmic baryon fraction  $f_b \equiv \Omega_b/\Omega_m$  and DM halo mass function (HMF) are known, since the total stellar mass cannot exceed the available baryonic mass. Applying this “baryon availability” argument, Boylan-Kolchin (2023) argued that within the  $\Lambda$ CDM cosmological model the population of high- $z$  galaxies of Labbé et al. (2023) can only be accommodated if the baryon-to-star conversion efficiency  $\epsilon$  is implausibly high, close to the theoretical upper bound

$\epsilon = 1$ . Stated differently, within  $\Lambda$ CDM the population of galaxies identified by Labbé et al. (2023) appears too abundant, too massive, and too early.

The above results were driven by early JWST imaging photometry, and are therefore subject to the intrinsic limitations of photometric redshift estimation and spectral energy distribution (SED)-based stellar mass determinations, motivating spectroscopic follow-up. Spectroscopic observations from the JWST First Reionization Epoch Spectroscopically Complete Observations (FRESCO) NIRCcam/grism survey have now provided secure redshifts for a sample of massive galaxies at  $5 \lesssim z \lesssim 9$  (Xiao et al. 2024). Under conservative assumptions, the properties of three ultra-massive galaxies in the FRESCO sample imply unusually high baryon-to-star conversion efficiencies of order  $\epsilon \sim 0.5$  (Xiao et al. 2024). This value is significantly larger than typical expectations, which typically indicate efficiencies  $\epsilon \lesssim 0.2$  level or lower, even at higher redshifts (Conroy & Wechsler 2009; Bigiel et al. 2008; Leroy et al. 2008; Kennicutt & Evans 2012; Moster et al. 2013; Behroozi et al. 2013a,b; Wechsler & Tinker 2018; Tacchella et al. 2018; Shuntov et al. 2022).<sup>1</sup> FRESCO spectroscopy therefore not only qualitatively confirms the trend suggested by CEERS photometry, but also places it on a firmer footing by providing secure redshifts and demonstrating that the efficiency problem is already present at lower redshifts (Xiao et al. 2024).

The above conclusions of Boylan-Kolchin (2023) and Xiao et al. (2024) were obtained from a “baryon availability” consistency argument based on direct comparison to theoretical bounds, checking whether individual extreme systems lay above or below theoretical predictions (assuming a  $\Lambda$ CDM cosmology with fixed parameters), rather than via a likelihood-based analysis. This approach, while simple and conservative, only really tests whether individual systems are consistent with theoretical expectations: it does not provide a probabilistic constraint on  $\epsilon$ , nor does it account for uncertainties in the underlying cosmological model and/or parameters. Given the potentially very important (astrophysical and cosmological) implications of these results, it is important to revisit the problem within a framework allowing for consistent comparison between data and theory, while accounting for uncertainties on the cosmological side. In this work we therefore move beyond the earlier fixed cosmological assumptions and per-object minimum-efficiency arguments, and perform

a full Bayesian analysis of most extreme galaxies within the CEERS and FRESCO samples. We do so not only within the spatially flat  $\Lambda$ CDM model, but also within some of its simplest extensions, for instance those with a free dark energy equation of state and/or spatial curvature. We stress that our goal is not that of ruling out  $\Lambda$ CDM, but rather to quantify, in a conservative and fully probabilistic manner, the range of baryon-to-star conversion efficiencies implied by current JWST observations once cosmological uncertainties are consistently accounted for. In short, we find that while CEERS provides only weak constraints and actually still allows relatively low efficiencies, FRESCO robustly favors relatively large efficiencies  $\epsilon \gtrsim 0.3$ – $0.5$  within all the cosmological extensions considered, suggesting that the origin of the “JWST tension” lies primarily in the efficiency of early star formation rather than in simple modifications of the background cosmology.

The rest of this paper is then organized as follows. In Sec. 2 we introduce the main observable used in this work (the cumulative comoving stellar mass density), and describe how theoretical predictions for this quantity depend on the underlying cosmology; we also present the four cosmological models considered in our analysis. In Sec. 3 we present the CEERS and FRESCO datasets and discuss the statistical framework adopted in our analysis. We present our results in Sec. 4, and critically discuss them in Sec. 5. We close in Sec. 6 by drawing concluding remarks.

## 2. FROM COSMOLOGICAL MODELS TO HIGH-REDSHIFT STELLAR MASS DENSITY

We now describe the procedure for obtaining theoretical predictions for the main observable used here, i.e. the cumulative comoving stellar mass density above a stellar mass threshold, which we denote by  $\rho_*( > M_*, z)$ . This observable, which we will refer to simply as “cumulative stellar mass density”, measures the total stellar mass per unit comoving volume contained in galaxies with stellar mass larger than a given value  $M_*$  at a given redshift.

To compute the *observed* cumulative stellar mass density, we specify a stellar mass threshold  $M_*$  within a redshift bin  $z \in [z_{\min}, z_{\max}]$ , and centered at an effective redshift  $z_{\text{eff}}$ . We then sum over the stellar masses of all galaxies which fall above the threshold, and divide by the survey comoving volume  $V$  (i.e. the comoving volume contained between  $z_{\min}$  and  $z_{\max}$ ), as follows:

$$\rho_*^{\text{obs}}(> M_*, z_{\text{eff}}) = \frac{1}{V} \sum_{M_i > M_*} M_i, \quad (1)$$

with  $M_i$  being the stellar masses of the individual galaxies above the threshold within the redshift bin. This

<sup>1</sup> See however Dekel et al. (2023); Boylan-Kolchin (2025); Shen et al. (2026) for studies suggesting mechanisms for increasing the efficiency of star formation at high redshifts.

definition agrees with the estimator adopted by [Boylan-Kolchin \(2023\)](#). Since the comoving volume depends on the assumed cosmology, the observable defined in Eq. (1) carries an implicit cosmological dependence which must be treated consistently when comparing observations against theoretical predictions, as we discuss in more detail later. For the purposes of our work, this observable presents several advantages. Firstly, it is by construction relatively insensitive to individual outliers or the properties of any single object, and instead captures the global abundance of massive systems. Additionally,  $\rho_*( > M_*, z)$  can be directly compared to theoretical cosmological upper bounds once the dark matter HMF and cosmic baryon fraction are known, without requiring detailed knowledge of galaxy formation physics or galaxy-halo matching prescriptions, as highlighted by [Boylan-Kolchin \(2023\)](#). Last but not least,  $\rho_*( > M_*, z)$  has already been used in earlier JWST-based “stress test” works (see for instance [Boylan-Kolchin 2023](#); [Xiao et al. 2024](#)), therefore facilitating direct comparisons.

In the standard picture of hierarchical structure formation, the abundance of DM halos is determined by the linear matter power spectrum and the growth history, and is measured by the DM halo mass function  $dn(M, z)/dM$ , i.e. the number of DM halos per unit mass per unit comoving volume at a given redshift. We follow the Sheth-Tormen prescription and compute the DM HMF as follows ([Sheth et al. 2001](#)):

$$\frac{dn(M, z)}{dM} = \frac{\bar{\rho}_m}{M} A \sqrt{\frac{2a}{\pi}} [1 + (av^2)^{-p}] \nu e^{-\frac{av^2}{2}} \left| \frac{d\nu}{dM} \right|. \quad (2)$$

In Eq. (2) above,  $\bar{\rho}_m = \Omega_m \rho_{\text{crit},0}$  is the mean comoving matter density, whereas  $\Omega_m$  and  $\rho_{\text{crit},0}$  are respectively the present-day matter density parameter and critical density. In our calculation we fix the Sheth-Tormen parameters to  $A = 0.3222$ ,  $a = 0.707$ , and  $p = 0.3$ . The peak height parameter is instead given by  $\nu = \delta_c / \sigma(M, z)$ , where  $\delta_c \simeq 1.686$  is the critical (linear) overdensity for collapse. Finally, we denote by  $\sigma(M, z)$  the root mean square linear matter fluctuation at redshift  $z$ , smoothed on the scale  $R = (3M/4\pi\bar{\rho}_m)^{1/3}$ :

$$\sigma^2(M, z) = D^2(z) \int \frac{dk}{2\pi^2} k^2 P(k) W^2(kR). \quad (3)$$

In Eq. (3) above,  $P(k)$  is the linear matter power spectrum at  $z = 0$ ,  $D(z)$  is the linear growth factor normalized such that  $D(0) = 1$ , and  $W(kR)$  is the Fourier transform of a real-space top-hat filter of radius  $R$ .

We then compute the cumulative comoving DM halo mass density contained in halos more massive than a

threshold  $M_{\text{halo}}$  from the DM HMF as follows:

$$\rho_m(> M_{\text{halo}}, z) = \int_{M_{\text{halo}}}^{\infty} dM M \frac{dn(M, z)}{dM}. \quad (4)$$

In order to connect Eq. (4) to the statistics of galaxies, we need a map between  $M_{\text{halo}}$  and the stellar content of a given halo,  $M_*$ . It is obvious that the cosmic baryon fraction  $f_b \equiv \Omega_b / \Omega_m$  (where  $\Omega_b$  is the present-day baryon density parameter) controls the maximum possible value of  $M_*$ . Following [Boylan-Kolchin \(2023\)](#), we parametrize the relation between  $M_*$  and  $M_{\text{halo}}$  as  $M_* = \epsilon f_b M_{\text{halo}}$ , where  $\epsilon \leq 1$  is a dimensionless parameter which quantifies the efficiency for converting gas into stars. Stated differently, we are assuming that only a fraction  $\epsilon$  of the available baryonic mass is converted into stars. We can then express the (theoretical) cumulative stellar mass density as follows:

$$\begin{aligned} \rho_*^{\text{th}}(> M_*, z) &= \epsilon f_b \rho_m \left( > \frac{M_*}{\epsilon f_b}, z \right) \\ &= \epsilon f_b \int_{\frac{M_*}{\epsilon f_b}}^{\infty} dM M \frac{dn(M, z)}{dM}. \end{aligned} \quad (5)$$

Given a certain value of  $\epsilon \leq 1$ , consistency between theory and observations requires that the following holds:

$$\rho_*^{\text{obs}}(> M_*, z_{\text{eff}}) \leq \rho_*^{\text{th}}(> M_*, z_{\text{eff}}). \quad (6)$$

The above condition is precisely the “baryon availability” argument introduced in [Boylan-Kolchin \(2023\)](#) (and also used in [Xiao et al. 2024](#)). This provides a conservative consistency test between observed galaxy properties and theoretical predictions for the halo population within a given cosmological model. In [Boylan-Kolchin \(2023\)](#) this stress test was performed in the limiting case  $\epsilon = 1$ , and other two (discrete) values of  $\epsilon$ . The  $\epsilon = 1$  case corresponds to the (theoretically allowed but otherwise extreme and rather implausible) scenario of complete conversion of all available baryons into stars, which sets an absolute upper bound on the allowed cumulative stellar mass density. Here we instead choose to treat  $\epsilon$  as a free parameter. As stressed above, the consistency condition set by Eq. (6) conservatively compresses all the uncertainties associated to galaxy formation physics into a single parameter  $\epsilon$ . The underlying cosmological model instead enters our theoretical prediction through both the expansion history and the growth of structure, see Eq. (5). In our analysis, we will compare different cosmological models while fixing the present-day amplitude of fluctuations, controlled by  $\sigma_8$ . As we shall see, it follows that what matters is the relative growth of perturbations with respect to today, a subtle point to which we return later.

We now introduce the four cosmological models considered in our later analysis. In order of increasing complexity, these models are:

- the concordance flat  $\Lambda$ CDM model, which represents our baseline model, and where dark energy (DE) takes the form of a cosmological constant with equation of state (EoS)  $w = -1$ ;
- the flat  $w$ CDM model, where the DE EoS takes values  $w \neq -1$ , while still remaining constant: this is one of the simplest extensions of our baseline model (see for instance Vagnozzi 2020; Escamilla et al. 2024; Luongo & Muccino 2024; Sammut 2025; Yadav et al. 2025, for recent examples of constraints on this model);
- the non-flat  $\Lambda$ CDM model, also referred to as  $o\Lambda$ CDM model, which allows for non-zero spatial curvature, characterized by a spatial curvature parameter  $\Omega_K \neq 0$ ; <sup>2</sup>;
- finally, the non-flat  $w$ CDM model, also referred to as  $ow$ CDM model, where  $w \neq -1$  and  $\Omega_K \neq 0$  simultaneously.

The last three models are among the simplest, best studied extensions to the concordance  $\Lambda$ CDM model (see for instance Di Valentino et al. 2025). In the context of the present work, they provide a minimal set of controlled extensions which allow us to study how departures from flat  $\Lambda$ CDM affect the abundance of high- $z$  massive DM halos and galaxies. The expansion history within each model is characterized by the dimensionless expansion rate  $E(z) \equiv H(z)/H_0$ , where  $H(z)$  and  $H_0$  are the Hubble rate and Hubble constant respectively. For the flat  $\Lambda$ CDM model  $E(z)$  is given as follows:

$$E_{\Lambda\text{CDM}}^2(z) = \Omega_m(1+z)^3 + \Omega_r(1+z)^4 + \Omega_\Lambda, \quad (7)$$

where  $\Omega_r$  is the radiation density parameter, and  $\Omega_\Lambda$  is the present-day cosmological constant density parameter. For the flat  $w$ CDM model,  $E(z)$  is instead given by

the following:

$$E_{w\text{CDM}}^2(z) = \Omega_m(1+z)^3 + \Omega_r(1+z)^4 + \Omega_{\text{DE}}(1+z)^{3(1+w)}, \quad (8)$$

where  $\Omega_{\text{DE}}$  is the present-day DE density parameter. For the non-flat  $\Lambda$ CDM model,  $E(z)$  is given as follows:

$$E_{o\Lambda\text{CDM}}^2(z) = E_{\Lambda\text{CDM}}^2(z) + \Omega_K(1+z)^2, \quad (9)$$

where  $\Omega_K$  is the present-day spatial curvature density parameter. Finally, in the non-flat  $w$ CDM model,  $E(z)$  is given by the following:

$$E_{ow\text{CDM}}^2(z) = E_{w\text{CDM}}^2 + \Omega_K(1+z)^2. \quad (10)$$

For all four models we neglect the radiation component, which is completely subdominant at the relevant epochs. The closure relation therefore implies that  $\Omega_\Lambda \approx 1 - \Omega_m$  within the flat  $\Lambda$ CDM model,  $\Omega_{\text{DE}} \approx 1 - \Omega_m$  within the flat  $w$ CDM model,  $\Omega_\Lambda \approx 1 - \Omega_m - \Omega_K$  within the non-flat  $\Lambda$ CDM model, and  $\Omega_{\text{DE}} \approx 1 - \Omega_m - \Omega_K$  within the non-flat  $w$ CDM model. When we introduce non-zero spatial curvature, we therefore implicitly compare different models at fixed  $\Omega_m$ , with the remaining energy budget redistributed between spatial curvature and the dark energy sector. Moreover, within all four models we can divide the matter sector into a cold DM and a baryon component, i.e.  $\Omega_m = \Omega_c + \Omega_b$ . We then define the cosmic baryon fraction as  $f_b = \Omega_b/\Omega_m$ .

The cosmological dependence of our theoretical predictions for the cumulative stellar mass density in Eq. (5) enters primarily through the linear growth factor  $D(z)$ , which determines the amplitude of matter fluctuations at the redshifts probed by JWST, and is itself controlled by the background expansion rate. In our analysis, we will compare different cosmological models at fixed  $\sigma_8$  and  $H_0$ . Stated differently, we fix both the present-day normalization of density fluctuations (and not their primordial amplitude), as well as the present-day expansion rate. The relevant quantity controlling the DM HMF is therefore the linear growth factor relative to its present-day value, given that the amplitude of matter fluctuations at redshift  $z$  can be expressed in the following way:

$$\sigma(M, z) = \sigma(M, 0) \frac{D(z)}{D(0)} = \sigma(M, 0) D(z), \quad (11)$$

where we adopt the conventional normalization  $D(0) = 1$ . Because models are compared *at fixed*  $\sigma_8$ , it is the growth *with respect to today* that matters, leading to a somewhat counterintuitive behaviour. Consider for instance a quintessence-like DE scenario with  $w > -1$ . If we fix  $H_0$ , the high-redshift expansion rate increases relative to  $\Lambda$ CDM. This increases the friction term in the

<sup>2</sup> See for instance Handley (2021); Wang et al. (2020); Di Valentino et al. (2019); Efstathiou & Gratton (2020); Di Valentino et al. (2021b); Chudaykin et al. (2021); Benisty & Staicova (2021); Vagnozzi et al. (2021a,b); Di Valentino et al. (2021a); Yang et al. (2021); Cao et al. (2021); Dhawan et al. (2021); Gonzalez et al. (2021); Dinda (2022); Zuckerman & Anchordoqui (2022); Bargiacchi et al. (2022); Akarsu et al. (2023); Glanville et al. (2022); Bel et al. (2022); Wu et al. (2023); Yang et al. (2023); Stevens et al. (2023); Favale et al. (2023); Qi et al. (2023); Giare et al. (2024); Wu & Zhang (2025); Liu et al. (2025); Forconi & Di Valentino (2025); Specogna et al. (2025) for recent examples of constraints on spatial curvature.

growth equation for matter overdensities  $\delta$ , and therefore slows the growth of structure. This implies that the amplitude of fluctuations at higher redshifts had to be larger in order to reach the same value today, given that we have chosen to fix  $\sigma_8$ . To put it differently, imagine evolving the system backwards from  $D(0) = 1$ . Then we would find that  $D(z)$  is larger relative to  $\Lambda$ CDM, which directly implies a larger abundance of high-redshift DM halos. Analogous considerations hold for a spatially open Universe ( $\Omega_K > 0$ ). The converse is true for models which (at fixed  $H_0$ ) reduce the expansion rate at high redshift relative to  $\Lambda$ CDM: in our case, this corresponds to phantom DE models (i.e. those with  $w < -1$ ) and a spatially closed Universe ( $\Omega_K < 0$ ), which therefore accelerate the growth of structure, and correspondingly suppress the abundance of DM halos at high redshift.

These points are illustrated in Fig. 1, where we plot the *maximum* allowed cumulative stellar mass density as a function of stellar mass predicted within different cosmological models, showing the impact of changing the DE EoS  $w$  (left panel) and the spatial curvature parameter  $\Omega_K$  (right panel). To compute the underlying DM HMF we adopt the Python package `hmf` (Murray et al. 2013), relying on the `astropy` library (Robitaille et al. 2013). The datapoints correspond to the CEERS cumulative stellar mass density measurements at  $z_{\text{eff}} \simeq 9.1$  (which have also been used in Boylan-Kolchin 2023), and are recomputed for each cosmology considered to consistently account for the fiducial cosmology dependence of the inferred cumulative stellar mass density and stellar masses, as discussed later in Sec. 3.1. The curves correspond to the limiting case  $\epsilon = 1$ , and thus represent the upper envelope of the cumulative stellar mass density allowed by each cosmological model within the ‘‘baryon availability’’ argument. In this limiting case, the quantity appearing on the  $x$  axis is therefore given by  $M_\star = f_b M_{\text{halo}}$ . We immediately observe that models with  $w > -1$  ( $w < -1$ ) enhance (suppress) the abundance of high-redshift halos and galaxies relative to the reference  $\Lambda$ CDM model, and similarly for models with  $\Omega_K > 0$  ( $\Omega_K < 0$ ), consistently with our earlier discussion. The differences between the curves directly reflect how changes in the background expansion history  $E(z)$  modify the relative growth factor  $D(z)/D(0)$ . We stress once more that the different models are being compared at fixed  $\Omega_m$ ,  $\sigma_8$ , and  $H_0$ , and the baryon fraction  $f_b$  is similarly fixed to  $f_b \simeq 0.15$ .

### 3. DATASETS AND METHODOLOGY

Having described how our theoretical predictions for the cumulative stellar mass density are obtained, we now introduce the data adopted in our later analysis,

as well as the statistical methods used to compare the data against theoretical predictions.

#### 3.1. Data

The *CEERS* dataset is based on early JWST multi-band imaging obtained with the NIRCcam as part of the CEERS program, which covers an effective survey area of  $\sim 40 \text{ arcmin}^2$ . Within this dataset, Labbé et al. (2023) identified a population of extremely massive, intrinsically red galaxy candidates with photometric redshifts  $6 \lesssim z \lesssim 10$ . We focus in particular on the highest redshift bin considered by Boylan-Kolchin (2023), containing galaxies with photometric redshifts  $8.5 < z < 10$ , and centered at an effective redshift  $z_{\text{eff}} \simeq 9.1$ . The individual galaxy properties are given in the upper three rows of Tab. 1. We compute the cumulative stellar mass density following Boylan-Kolchin (2023) and considering the three most extreme systems, with the stellar masses of the two most extreme ones exceeding  $10^{10} M_\odot$ . Following Eq. (1), we evaluate  $\rho_\star^{\text{obs}}(> M_\star, z_{\text{eff}} = 9.1)$  at the two thresholds reported in Boylan-Kolchin (2023). We obtain values of order  $\rho_\star \lesssim 10^6 M_\odot \text{Mpc}^{-3}$ , in agreement with those reported by Boylan-Kolchin (2023). Only the most massive object contributes to the highest mass bin, whereas all three objects contribute to the lowest mass bin. These two measurements of  $\rho_\star^{\text{obs}}$ , which are also those reported in Fig. 1, define the CEERS datapoints which enter the likelihood adopted in our later statistical analysis. The uncertainties are computed following Labbé et al. (2023), and reflect both Poisson statistics and cosmic variance. We stress that, since the CEERS sample is based on photometric redshifts and stellar mass estimates, the resulting cumulative stellar mass density measurements carry substantial uncertainties. We expect this to translate into rather loose constraints on  $\epsilon$ , as our full Bayesian analysis will confirm.

The *FRESCO* dataset is based on JWST NIRCam/grism spectroscopy obtained within the FRESCO program, covering a total survey area of  $\sim 124 \text{ arcmin}^2$  across the GOODS-North and GOODS-South fields. Within the survey, Xiao et al. (2024) identified a population of spectroscopically confirmed extremely massive, red, emission-line galaxies, many of which had been missed by earlier UV-selected surveys due to heavy dust obscuration. The spectroscopic redshifts of these galaxies fall in the range  $5 \lesssim z \lesssim 9$ . Following Xiao et al. (2024), we focus on the lowest redshift bin  $5 < z < 6$  centered at an effective redshift  $z_{\text{eff}} \simeq 5.5$ , since the stellar masses derived for galaxies in this bin are significantly more robust than those of galaxies at higher redshifts. The individual galaxy properties are given in the lower three rows of Tab. 1. We compute the cumu-

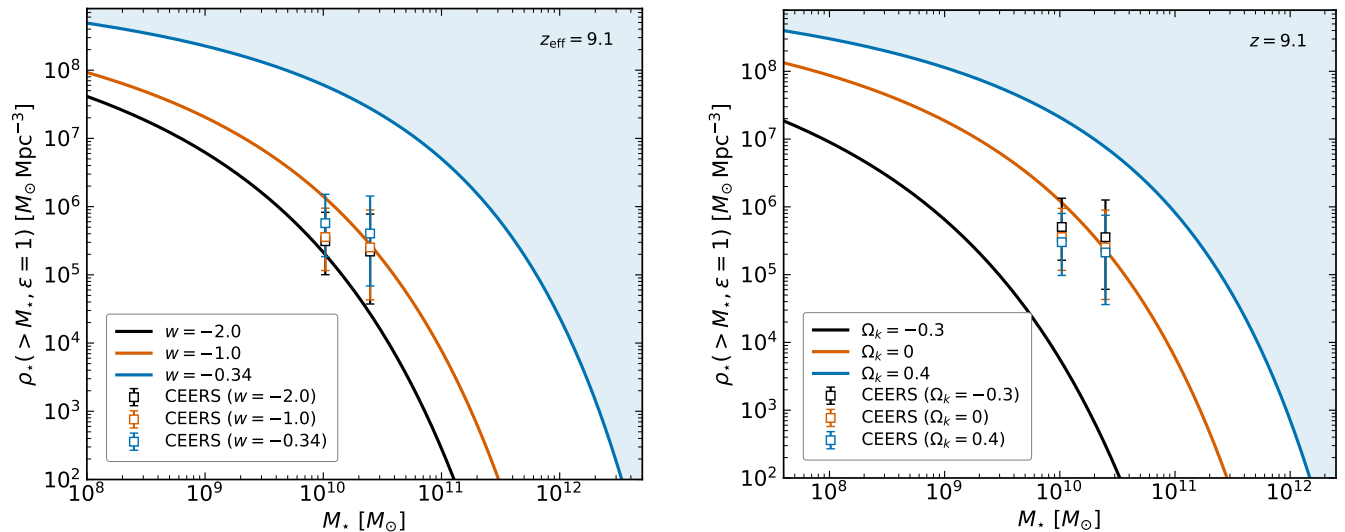


**Figure 1.** Maximum allowed cumulative comoving stellar mass density as a function of stellar mass predicted within different cosmological models, compared at fixed  $\Omega_m$ ,  $\sigma_8$ , and  $H_0$ , with baryon fraction fixed to  $f_b \simeq 0.15$ . The curves correspond to the limiting case  $\epsilon = 1$ , and thus represent the upper envelope of the cumulative stellar mass density allowed by each cosmological model within the “baryon availability” argument (the blue shaded region is excluded by the “baryon availability” argument in the most generous case). The datapoints correspond to the CEERS measurements at  $z_{\text{eff}} \simeq 9.1$ , and are recomputed for each cosmology considered to consistently account for the fiducial cosmology dependence of the inferred cumulative stellar mass density and stellar masses. *Left panel:* comparison between models with different values of the dark energy equation of state  $w = -1$  ( $\Lambda$ CDM, orange curve),  $-0.34$  (blue curve), and  $-2.0$  (black curve). We clearly see that, at fixed  $\sigma_8$ , quintessence-like (phantom) models with  $w > -1$  ( $w < -1$ ) enhance (suppress) the abundance of high-redshift galaxies relative to  $\Lambda$ CDM. *Right panel:* comparison between models with different values of the spatial curvature parameter  $\Omega_K = 0$  ( $\Lambda$ CDM, orange curve),  $0.4$  (blue curve), and  $-0.3$  (black curve). We clearly see that, at fixed  $\Omega_m$  (with the difference in energy density implied by spatial curvature being accounted for by the dark energy sector), spatially open (closed) models with  $\Omega_K > 0$  ( $\Omega_K < 0$ ) enhance (suppress) the abundance of high-redshift galaxies relative to  $\Lambda$ CDM.

relative stellar mass density by considering the three most extreme objects in this redshift bin, named  $S1$ ,  $S2$ , and  $S3$ , whose masses exceed  $10^{11} M_\odot$  (Xiao et al. 2024). We then evaluate  $\rho_*^{\text{obs}}(> M_*, z_{\text{eff}} = 5.5)$  at three stellar mass thresholds:  $M_* = 1.096 \times 10^{11} M_\odot$ ,  $1.514 \times 10^{11} M_\odot$ , and  $2.344 \times 10^{11} M_\odot$ . We note that all three galaxies contribute above the first threshold, whereas only  $S2$  and  $S1$  contribute above the second, and only  $S1$  contributes above the third. This yields cumulative stellar mass densities of order  $\rho_* \lesssim 10^6 M_\odot \text{Mpc}^{-3}$ . These three measurements of  $\rho_*^{\text{obs}}$  define the FRESCO datapoints which enter the likelihood adopted in our later statistical analysis, and their uncertainties reflect both Poisson statistics and cosmic variance. Owing to the spectroscopic confirmation of the galaxies and, accordingly, the more robust redshift and stellar mass estimates, the FRESCO measurements have substantially smaller relative uncertainties compared to their CEERS counterparts. We therefore expect them to lead to significantly tighter limits on  $\epsilon$ , as our analysis will confirm.

We stress that the observed value of  $\rho_*^{\text{obs}}(> M_*)$  depends on an assumed fiducial cosmology in two different ways (see Menci et al. 2022, 2024a, for discussions). In

first place, since stellar masses derived from photometric observations are inferred from observed fluxes, they scale with luminosity distance as  $M_* \propto d_L^2$ . This is true even for galaxies with spectroscopic redshifts such as the FRESCO ones, given that their stellar masses are still derived from SED modelling and therefore follow the same scaling. Moreover, as Eq. (1) makes explicit, the cumulative stellar mass density depend on the comoving survey volume: this is a cosmology-dependent quantity, as computing requires assuming a specific expansion history to compute the distance-redshift relation, i.e. a fiducial cosmology. These issues were not relevant to the earlier works of Boylan-Kolchin (2023) and Xiao et al. (2024), since they worked at fixed cosmology, but are essential when conducting a full Bayesian analysis scanning over different cosmologies, as we aim to do here. Therefore, at each step of our Monte Carlo Markov Chain (MCMC) analysis, we will rescale  $\rho_*^{\text{obs}}$  by the ratio of the comoving volume within the fiducial cosmology to that in the cosmology at the given MCMC step. The assumed fiducial cosmology is the best-fit *Planck* 2018  $\Lambda$ CDM cosmological model, with  $H_0 = 67.4 \text{ km/s/Mpc}$ ,  $\Omega_m = 0.315$ , and  $\sigma_8 = 0.811$  (Aghanim et al. 2020).

Dataset	ID	$z$	$\log_{10}(M_*/M_\odot)$
CEERS	35300	9.08	10.40
CEERS	14924	8.83	10.02
CEERS	21834	8.54	9.61
FRESCO	S-18258 (S1)	5.58	11.37
FRESCO	N-7496 (S2/GN10)	5.31	11.18
FRESCO	N-2663 (S3)	5.18	11.04

**Table 1.** Properties of the most extreme galaxies used to compute the cumulative stellar mass densities for the CEERS and FRESCO datasets. For each galaxy, we report the catalog identifier, redshift (photometric redshifts for CEERS, spectroscopic redshifts for FRESCO), and (logarithm of the) stellar mass in units of solar masses. For the FRESCO dataset, we report both the catalog identifiers and the labels (S1, S2, S3) used in Xiao et al. (2024); note that S2 is also known as GN10 in the literature. Stellar masses correspond to values inferred from SED fitting assuming the fiducial cosmology.

Similarly, the values of  $M_*$  at each MCMC step are rescaled by the square of the ratio of the luminosity distance within the cosmology at the given MCMC step to that in the fiducial cosmology.

### 3.2. Statistical framework

For each of the four models studied, characterized by the unnormalized expansion rates given in Eqs. (7–10), the baseline set of parameters is given by the matter density parameter  $\Omega_m$ , the present-day amplitude of fluctuations  $\sigma_8$ , and the baryon-to-star conversion efficiency  $\epsilon$ . We have explicitly checked that the physical matter density  $\omega_b$  and the Hubble constant  $H_0$  do not have a strong impact on the predicted cumulative stellar mass density, and therefore opt to fix these parameters to  $\omega_b = 0.02233$  and  $H_0 = 67.4$  km/s/Mpc respectively (Aghanim et al. 2020). We note that both  $\omega_b$  and  $H_0$  are required to compute the cosmic baryon fraction  $f_b \equiv \Omega_b/\Omega_m = \omega_b/\Omega_m h^2$ , which enters the theoretical prediction for the cumulative stellar mass density as in Eq. (5), and is consistently computed at each step of our MCMC analysis to account for the different values of  $\Omega_m$  we sample. For our purposes the flat  $\Lambda$ CDM model parameter space is therefore 3-dimensional, and described by the parameter vector  $\{\Omega_m, \sigma_8, \epsilon\}$ . Similarly, the 4-dimensional flat  $w$ CDM and non-flat  $\Lambda$ CDM models are described by the parameter vectors  $\{\Omega_m, \sigma_8, \epsilon, w\}$  and  $\{\Omega_m, \sigma_8, \epsilon, \Omega_K\}$  respectively. Finally, the 5-dimensional non-flat  $w$ CDM model is described by the parameter vector  $\{\Omega_m, \sigma_8, \epsilon, w, \Omega_K\}$ .

We sample the posterior distributions of the four cosmological models running MCMC chains through the `emcee` sampler (Foreman-Mackey et al. 2013). Predictions for the HMF within each model are obtained through the publicly available Python package `hmf` (Murray et al. 2013), which relies on the `astropy` library (Robitaille et al. 2013). For each model, we evolve an ensemble of  $N_w = 8$  walkers for  $N_{\text{step}} = 10000$  steps (except for the non-flat  $w$ CDM model, for which

we use 18000 steps), and conservatively discard the first 2000 points of each chain as burn-in. We assess the convergence of the chains by estimating the integrated autocorrelation time  $\tau$  for each parameter, and verifying that the chain length satisfies  $N_{\text{step}} \gg 50\tau$ . We confirm that the total number of independent samples,  $N_{\text{ind}} \simeq N_w N_{\text{step}}/\tau$ , exceeds by far  $\sim 10^3$  for all parameters. We then analyze the resulting MCMC chains using the `GetDist` package (Lewis 2025).

We set wide, flat priors on all three cosmological parameters, verifying a posteriori that our posteriors are not affected by the choice of prior bounds. In particular, we set uniform prior ranges on  $\sigma_8 \in [0.76, 0.84]$ ,  $\epsilon \in [0.01, 1.00]$ ,  $w \in [-2.00, -0.33]$ , and  $\Omega_K \in [-0.2, 0.4]$ , all of which are very broad and consistent with the constraints imposed from independent cosmological probes. In particular, for what concerns  $\epsilon$ , we do not allow the prior range to go all the way down to  $\epsilon = 0$  since in that limit the cumulative stellar mass density is identically zero, and therefore in obvious disagreement with data. As for  $w$ , the upper limit of  $w = -0.33$  is set by the requirement that the DE component should drive cosmic acceleration, which requires  $w < -1/3$ .

For the matter density parameter  $\Omega_m$ , following the reasoning of Pedrotti et al. (2026) we set a Gaussian prior  $\Omega_m = 0.30 \pm 0.03$ . This prior reflects the fact that  $\Omega_m$  is very well constrained by a wide variety of late-time probes. At the same time, there remains a mild level of disagreement between different datasets (Sakr 2023; Akarsu et al. 2024; Pedrotti et al. 2025; Colgáin & Sheikh-Jabbari 2025; Lynch & Knox 2025; Lee 2026, 2025; Wang et al. 2025; Weiner 2026; Shlivko & Poulin 2026), with *DESI* BAO measurements indicating lower values  $\Omega_m \sim 0.28$  (Adame et al. 2025; Abdul Karim et al. 2025; Chudaykin et al. 2026), whereas several Type Ia Supernovae datasets indicate somewhat larger values  $\Omega_m \gtrsim 0.33$  (Rubin et al. 2025; Abbott et al. 2024; Baryakhtar et al. 2024; Colgáin et al. 2025a). Even accounting for this spread across different probes, it is clear

that extreme values such as  $\Omega_m \lesssim 0.25$  and  $\Omega_m \gtrsim 0.35$  are strongly disfavored by virtually all datasets. Our choice of prior is therefore conservative, in the sense that its rather generous width more than reflects the current spread among different determinations of  $\Omega_m$ , while its central value is not tied to any single measurement (although it is consistent with the model-independent “un-calibrated cosmic standards” determinations of [Lin et al. 2021](#); [Wang & Lin 2025](#)).

We adopt a one-sided semi-Gaussian likelihood. Denoting by  $\theta$  the parameter vector sampled in our MCMC, the log-likelihood takes the following form:

$$-\ln \mathcal{L}(\theta) = \frac{1}{2} \sum_i \begin{cases} \frac{[\rho_{\star,i}^{\text{th}}(\theta) - \rho_{\star,i}^{\text{obs}}]^2}{\sigma_i^2} & (\rho_{\star,i}^{\text{th}}(\theta) < \rho_{\star,i}^{\text{obs}}) \\ 0 & (\rho_{\star,i}^{\text{th}}(\theta) \geq \rho_{\star,i}^{\text{obs}}) \end{cases} \quad (12)$$

where the sum runs over the different cumulative stellar mass density measurements (two for CEERS and three for FRESCO), and  $\sigma_i$  are the associated observational uncertainties. The rationale behind the semi-Gaussian likelihood mirrors that of [Vagnozzi et al. \(2022\)](#); [Wei & Melia \(2022\)](#); [Binici et al. \(2024\)](#), and is as follows. Parameters predicting cumulative stellar mass densities smaller than the observed ones should be penalized according to a Gaussian likelihood, i.e. exponentially suppressed as the discrepancy increases. On the other hand, parameters predicting larger values of the cumulative stellar mass density compared to the observed ones should not be penalized (although see the discussion in [Costa et al. 2023](#)). The reason is that the observed cumulative stellar mass density should be interpreted conservatively, because incompleteness and selection effects may lead to an underestimation of the true abundance of massive galaxies. A symmetric Gaussian likelihood would instead artificially strengthen the obtained constraints unless such effects were modeled explicitly, which is beyond the scope of this work. Our semi-Gaussian likelihood can be viewed as a continuous generalization of the binary “baryon availability” stress test carried out by [Boylan-Kolchin \(2023\)](#), in which models either pass or fail depending on whether they can predict a cumulative stellar mass density at least as large as observed. Our treatment implements the same logic in the sense that parameters failing the consistency condition are penalized, whereas parameters satisfying it are not required to precisely match the observed values.

From our posterior distributions we derive one-sided lower limits on  $\epsilon$ , quoting 68% and 95% one-sided lower limits, which correspond to the 32<sup>nd</sup> and 5<sup>th</sup> percentiles

of the posterior distributions.<sup>3</sup> We also quantify the statistical significance at which a given reference value of  $\epsilon = \epsilon_0$  is excluded, computing the posterior probability  $p = P(\epsilon < \epsilon_0)$  from the fraction of MCMC samples satisfying the condition  $\epsilon < \epsilon_0$ . We convert this to a Gaussian-equivalent one-sided significance  $Z$  by computing the corresponding one-sided tail probability for a standard normal distribution as  $Z = \Phi^{-1}(1 - p)$ , where  $\Phi$  is the cumulative distribution function of the unit normal distribution. The benchmark reference value we choose is  $\epsilon_0 = 0.2$ : this is a relatively high conversion efficiency, yet one which is still consistent with upper estimates from empirical stellar-to-halo mass relations ([Conroy & Wechsler 2009](#); [Bigiel et al. 2008](#); [Leroy et al. 2008](#); [Kennicutt & Evans 2012](#); [Moster et al. 2013](#); [Behroozi et al. 2013a,b](#); [Wechsler & Tinker 2018](#); [Tacchella et al. 2018](#); [Shuntov et al. 2022](#)). Values  $\epsilon \gtrsim 0.2$  therefore already imply very efficient star formation, and the statistical significance at which  $\epsilon = 0.2$  is excluded provides a conservative but meaningful measure of the tension with standard galaxy formation scenarios. For completeness, we also consider values of  $\epsilon_0 = 0.1$  and 0.15, noting that the former value allows for a direct comparison with the results of [Boylan-Kolchin \(2023\)](#).

#### 4. RESULTS

We begin with a brief anticipation of our main results before discussing them in detail. We find that the CEERS dataset mildly favors high values of  $\epsilon$ , but the comparatively large uncertainties imply that lower, astrophysically more plausible values of  $\epsilon$  remain consistent. On the other hand, the FRESCO dataset requires significantly larger values of  $\epsilon \gtrsim 0.5 - 0.7$  within  $\Lambda$ CDM. Freeing up  $w$  or  $\Omega_K$  somewhat relaxes this requirement but does not eliminate the need for high values of  $\epsilon \gtrsim 0.3$  for extensions to  $\Lambda$ CDM. Overall, we find no evidence for deviations from  $\Lambda$ CDM, with  $w = -1$  and  $\Omega_K = 0$  remaining fully consistent with the data: this suggests

<sup>3</sup> All the limits we compute are one-sided as our likelihood penalizes only parameters whose corresponding cumulative stellar mass densities are too low. As a result, only sufficiently low values of  $\epsilon$  are statistically disfavored, and the posterior distribution of  $\epsilon$  is of the “limit-type” frequently encountered in cosmology, where only one side of the parameter space is constrained. See for instance the case of the sum of neutrino masses  $\sum m_\nu$ , for which upper limits are typically obtained, at least when the physical prior  $\sum m_\nu \geq 0$  eV is assumed ([Vagnozzi et al. 2017, 2018](#); [Roy Choudhury & Naskar 2019](#); [Roy Choudhury & Hannestad 2020](#); [Tanseri et al. 2022](#); [Wang et al. 2024a](#); [Green & Meyers 2025](#); [Naredo-Tuero et al. 2024](#); [Du et al. 2025](#); [Jiang et al. 2025b](#); [Roy Choudhury & Okumura 2024](#); [Loverde & Weiner 2024](#); [Roy Choudhury 2025](#); [Roy Choudhury et al. 2025](#); [Feng et al. 2026](#)).

that the tension is of astrophysical rather than cosmological nature.

#### 4.1. Flat $\Lambda$ CDM model

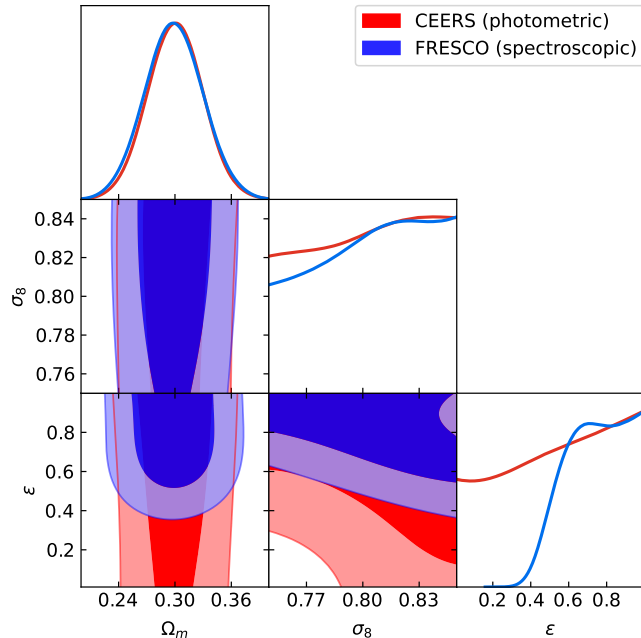


**Figure 2.** Triangular plot showing 2D joint and 1D marginalized posterior probability distributions for the present-day matter density parameter  $\Omega_m$ , the present-day amplitude of fluctuations  $\sigma_8$ , and baryon-to-star conversion efficiency  $\epsilon$ , obtained within the flat  $\Lambda$ CDM model in light of the photometric CEERS (red contours) and spectroscopic FRESKO (blue contours) samples. We note that the FRESKO constraints on  $\epsilon$  are significantly tighter than their CEERS counterparts, due to the comparatively larger uncertainties of the latter.

We begin by discussing the flat  $\Lambda$ CDM model, where we recall that the parameters being varied are  $\Omega_m$ ,  $\sigma_8$ , and  $\epsilon$ . The posterior distributions for these parameters are shown in Fig. 2, for both the CEERS (red) and FRESKO (blue) datasets.

For the CEERS dataset, we find the one-sided lower limits  $\epsilon \gtrsim 0.39$  and  $\epsilon \gtrsim 0.07$  at 68% and 95% C.L. respectively. For what concerns the baryon-to-star conversion efficiency, we find that our benchmark reference value  $\epsilon_0 = 0.2$  is consistent with the data within  $1.0\sigma$ , confirming that the constraints on  $\epsilon$  are relatively weak. Similarly, values of  $\epsilon_0 = 0.15$  and  $0.1$  are consistent with the data within  $1.2\sigma$  and  $1.4\sigma$  respectively. These results differ from those of [Boylan-Kolchin \(2023\)](#), where a stronger tension with  $\Lambda$ CDM was reported, prompting an ongoing discussion on whether high-redshift galaxies

observed by JWST call for new physics.<sup>4</sup> The origin of the discrepancy is entirely in the different choice of statistical methodology: a full Bayesian analysis marginalizing over cosmological parameters and properly accounting for observational uncertainties shows that the apparent tension is actually rather weak, since relatively low values of  $\epsilon$  remain statistically allowed because of the large uncertainties of the CEERS dataset.

In contrast, for the FRESKO dataset we find significantly stronger constraints, i.e.  $\epsilon \gtrsim 0.65$  and  $\epsilon \gtrsim 0.48$  at 68% and 95% C.L. respectively. These results, which are qualitatively consistent with those of [Xiao et al. \(2024\)](#) (while being obtained within a full Bayesian framework), point to a strong requirement for very efficient star formation in the early Universe within the flat  $\Lambda$ CDM model. We find that benchmark values of  $\epsilon_0 = 0.2$ ,  $0.15$ , and  $0.1$  are all disfavored by the data at a statistical significance of  $> 5\sigma$ .

For what concerns the cosmological parameters, we find that  $\Omega_m$  and  $\sigma_8$  are mostly prior dominated, with no significant shifts between the CEERS and FRESKO datasets. Furthermore, as is clear from the posterior distributions shown in Fig. 2, we observe mild degeneracies between  $\epsilon$  and  $\sigma_8$ . In particular, the two parameters exhibit a negative correlation, reflecting the fact that a reduction in the growth of structure can be compensated by a more efficient star formation. Nevertheless, this degeneracy is not sufficient to alleviate the strong preference for high values of  $\epsilon$  in the FRESKO case, as doing so would require implausibly high values of  $\sigma_8$ .

#### 4.2. Flat $w$ CDM model

We move on to the flat  $w$ CDM model, where the parameters being varied are  $\Omega_m$ ,  $\sigma_8$ ,  $\epsilon$ , and  $w$ . Their posterior distributions in light of both the CEERS and FRESKO datasets are shown in Fig. 3, with the same

<sup>4</sup> See for instance [Ferrara et al. \(2023\)](#); [Liu & Bromm \(2022\)](#); [Bi-agetti et al. \(2023\)](#); [Haslbauer et al. \(2022\)](#); [Hütsi et al. \(2023\)](#); [Gandolfi et al. \(2022\)](#); [Maio & Viel \(2023\)](#); [Wang & Liu \(2022\)](#); [Yuan et al. \(2024\)](#); [Dayal & Giri \(2024\)](#); [Ilie et al. \(2023\)](#); [Jiao et al. \(2023\)](#); [Parashari & Laha \(2023\)](#); [Lei et al. \(2024\)](#); [Shen et al. \(2023\)](#); [Qin et al. \(2023\)](#); [Padmanabhan & Loeb \(2023\)](#); [Su et al. \(2023\)](#); [Lin et al. \(2024\)](#); [Forconi et al. \(2023\)](#); [Guo et al. \(2024\)](#); [Huang et al. \(2024a\)](#); [Pallottini & Ferrara \(2023\)](#); [Bird et al. \(2024\)](#); [Wang et al. \(2024c, 2023\)](#); [Adil et al. \(2023\)](#); [Sun et al. \(2023\)](#); [Casey et al. \(2024\)](#); [Pacucci et al. \(2023\)](#); [Gupta \(2023\)](#); [Wang et al. \(2024b\)](#); [Forconi et al. \(2024\)](#); [van Putten \(2024\)](#); [Iocco & Visinelli \(2024\)](#); [Hegde et al. \(2024\)](#); [Colgáin et al. \(2025b\)](#); [Lu et al. \(2024\)](#); [Huang et al. \(2024b\)](#); [Jiang et al. \(2025a\)](#); [Menci et al. \(2024b\)](#); [Wang et al. \(2024d\)](#); [Lei et al. \(2025\)](#); [Ziegler et al. \(2025\)](#); [Fakhry et al. \(2025\)](#); [Lei et al. \(2026\)](#); [Zhou et al. \(2025\)](#); [Fakhry et al. \(2026\)](#); [Das et al. \(2025\)](#); [Menci et al. \(2026\)](#) for examples of various works investigating the implications of the JWST observations for fundamental physics and/or our understanding of galaxy formation.

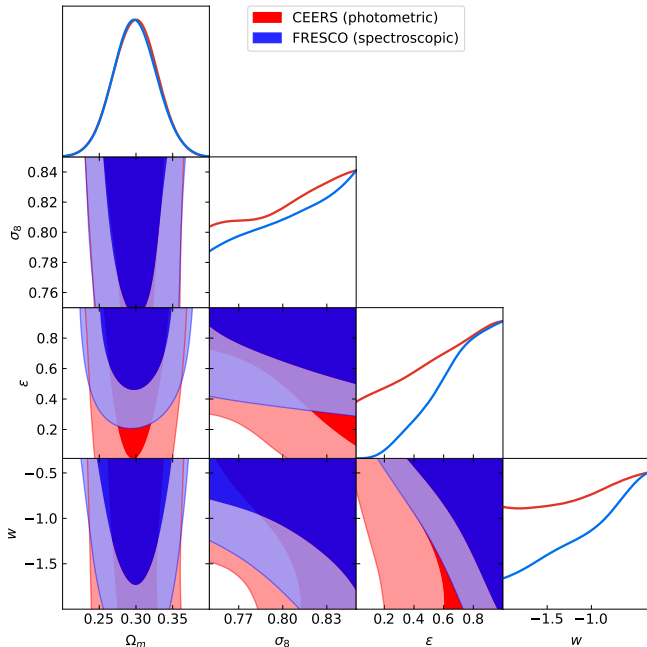


**Figure 3.** As in Fig. 2, but for the flat  $w$ CDM model, therefore including the dark energy equation of state  $w$  among the parameters.

color coding as earlier. Using the CEERS dataset, we derive the one-sided lower limits  $\epsilon \gtrsim 0.39$  and  $\epsilon \gtrsim 0.07$  at 68% and 95% C.L. respectively. Both figures are in very good agreement with their flat  $\Lambda$ CDM counterparts. Similarly, we find that the data is consistent with benchmark values  $\epsilon_0 = 0.2, 0.15,$  and  $0.1$  at the  $0.9\sigma, 1.1\sigma,$  and  $1.3\sigma$  levels respectively. This confirms that the constraints on  $\epsilon$  remain relatively weak. As we could have expected, the DE EoS remains poorly constrained, with  $w \gtrsim -1.41$  and  $w \gtrsim -1.91$  at 68% and 95% C.L. respectively, and a posterior probability for quintessence-like values of  $p(w > -1) = 0.45$ , indicating no evidence for deviations from a cosmological constant in the DE sector.

When instead considering the FRESCO dataset, the trend observed earlier in the flat  $\Lambda$ CDM model is fully confirmed. We find significantly stronger constraints of  $\epsilon \gtrsim 0.64$  and  $\epsilon \gtrsim 0.34$  at 68% and 95% C.L. respectively, whereas values of  $\epsilon_0 = 0.2, 0.15,$  and  $0.1$  are disfavored at the  $2.2\sigma, 3.5\sigma,$  and  $> 5\sigma$  levels respectively. This suggests that allowing  $w$  to vary somewhat relaxes the requirement of a very strong baryon-to-star conversion efficiency relative to flat  $\Lambda$ CDM, but is unable to eliminate the need for high efficiencies. Finally, for the DE EoS we infer  $w \gtrsim -1.18$  and  $w \gtrsim -1.81$  at 68% and 95% C.L., whereas the posterior probability for quintessence-like values is  $p(w > -1) = 0.57$ , again

showing no statistically significant evidence for deviations from the cosmological constant.

As one could have anticipated from our earlier discussion on the growth factor, there is a clear degeneracy between  $w$  and  $\epsilon$ , which again is reflected by a negative correlation between the two. The reason is that more quintessence-like values of  $w > -1$  increase the abundance of massive halos, therefore relaxing the requirement of high values of  $\epsilon$ , with the converse being true for phantom values of  $w < -1$ . Similar considerations hold for the degeneracy between  $w$  and  $\sigma_8$ , since changes in the expansion history also affect the normalization of structure growth. For the same reason, the introduction of  $w$  as a free parameter weakens the negative correlation between  $\epsilon$  and  $\sigma_8$  observed in flat  $\Lambda$ CDM or, more precisely, redistributes the earlier  $\epsilon$ - $\sigma_8$  degeneracy among  $\epsilon, w,$  and  $\sigma_8$ . Nevertheless, FRESCO data still require relatively high values of  $\epsilon$ , indicating that the simple modification of the expansion history we are considering is unable to resolve the tension, which is reflected in the absence of indications for deviations from the  $\Lambda$ CDM limit  $w = -1$ .

#### 4.3. Non-flat $\Lambda$ CDM model

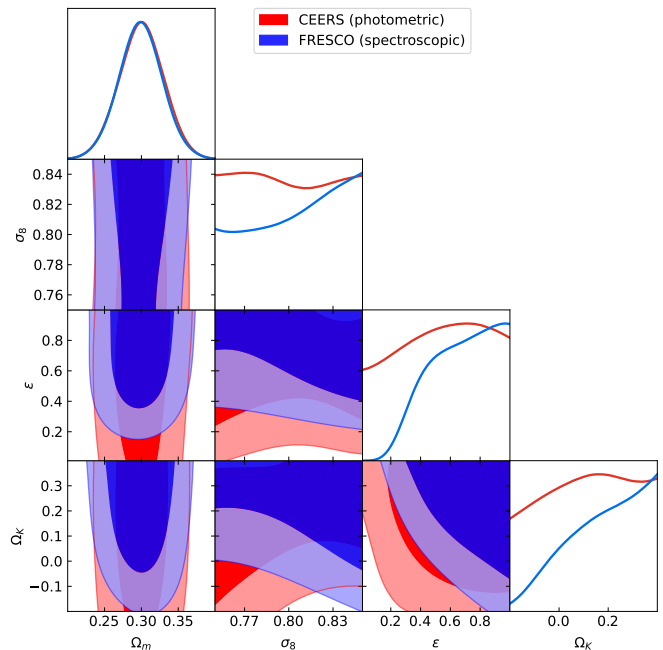


**Figure 4.** As in Fig. 2, but for the non-flat  $\Lambda$ CDM model, therefore including the spatial curvature parameter  $\Omega_K$  among the parameters.

We now study the non-flat  $\Lambda$ CDM model, where the parameters being varied are  $\Omega_m, \sigma_8, \epsilon,$  and  $\Omega_K$ . The corresponding posterior distributions are shown in Fig. 4.

For the CEERS dataset, we find one-sided lower limits  $\epsilon \gtrsim 0.38$  and  $\epsilon \gtrsim 0.07$  at 68% and 95% C.L. respectively, in very good agreement with the earlier flat  $\Lambda$ CDM results. The data is consistent with our benchmark values  $\epsilon_0 = 0.2, 0.15,$  and  $0.1$  at the  $0.9\sigma, 1.1\sigma,$  and  $1.3\sigma$  levels respectively. This again confirms that constraints on  $\epsilon$  are weak due to the relatively large uncertainties of the data. Similarly, we obtain comparatively weak constraints on the spatial curvature parameter, with one-sided lower limits of  $\Omega_K \gtrsim 0.02$  and  $\Omega_K \gtrsim -0.16$  at 68% and 95% C.L. respectively. The posterior probability for negative spatial curvature (i.e. positive spatial curvature parameter, corresponding to a spatially open Universe) is  $p(\Omega_K > 0) = 0.70$ , with no statistically significant preference for deviations from spatial flatness.

For the FRESCO dataset, we confirm the trends observed earlier in the flat  $\Lambda$ CDM and  $w$ CDM models. In particular, we find stronger constraints on the baryon-to-star conversion efficiency compared to those obtained with the CEERS sample, with  $\epsilon \gtrsim 0.55$  and  $\epsilon \gtrsim 0.30$  at 68% and 95% C.L. respectively, whereas our benchmark values of  $\epsilon_0 = 0.2, 0.15,$  and  $0.1$  are disfavored at the  $2.7\sigma, 3.6\sigma,$  and  $> 5\sigma$  levels respectively. This indicates that, while allowing for non-zero spatial curvature somewhat relaxes the constraints relative to flat  $\Lambda$ CDM, the requirement for very high efficiencies persists, similar to the trend observed when the DE EoS was freed. For the spatial curvature parameters, we find  $\Omega_K \gtrsim 0.11$  and  $\Omega_K \gtrsim -0.08$  at 68% and 95% C.L. respectively, with a posterior probability for negative spatial curvature  $p(\Omega_K > 0) = 0.85$ , corresponding to an extremely weak preference for an open Universe, one not worthy of further discussion.

Similarly to the flat  $w$ CDM model, we find that allowing for non-zero spatial curvature introduces a degeneracy between  $\Omega_K$  and  $\epsilon$ . This is reflected by a negative correlation between the two, since negative spatial curvature ( $\Omega_K > 0$ ) modifies the expansion history (albeit through its geometric contribution to the Friedmann equation rather than through a true dynamical component), and hence the growth of structure, in such a way as to enhance the latter at early times, which can be compensated by smaller baryon-to-star conversion efficiencies. Moreover, the introduction of  $\Omega_K$  as a free parameter redistributes the earlier  $\epsilon$ - $\sigma_8$  degeneracy among  $\epsilon, \Omega_K,$  and  $\sigma_8$ . Nevertheless, even allowing for non-zero spatial curvature, FRESCO data continue to require high values of  $\epsilon$ , and show no statistically significant indications for departures from spatial flatness.

#### 4.4. Non-flat $w$ CDM model

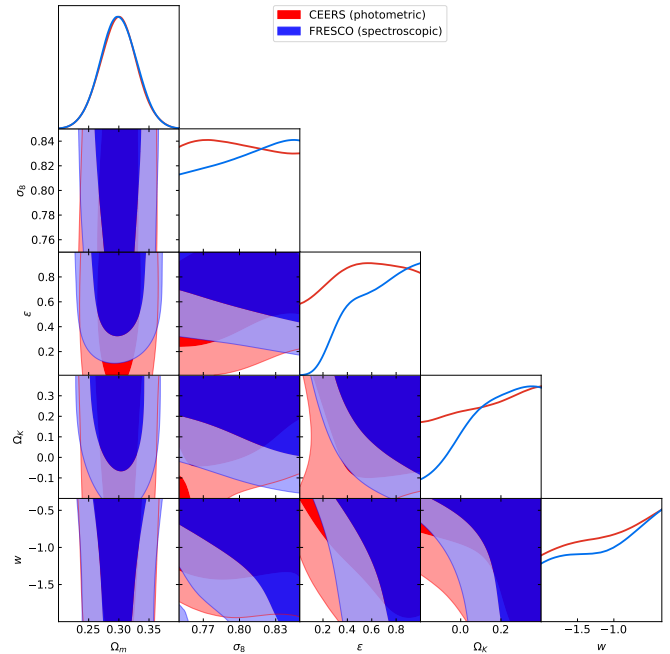


**Figure 5.** As in Fig. 2, but for the non-flat  $w$ CDM model, therefore including the dark energy equation of state  $w$  and spatial curvature parameter  $\Omega_K$  among the parameters.

The most general model we consider is the non-flat  $w$ CDM model, where the parameters being varied are  $\Omega_m, \sigma_8, \epsilon, w,$  and  $\Omega_K$ . The corresponding posterior distributions are shown in Fig. 5.

For the CEERS dataset, we find one-sided lower limits  $\epsilon \gtrsim 0.38$  and  $\epsilon \gtrsim 0.07$  at 68% and 95% C.L. respectively, in very good agreement with the results obtained in all previous models. We find the data to be in agreement with our benchmark values  $\epsilon_0 = 0.2, 0.15,$  and  $0.1$  at the  $0.9\sigma, 1.1\sigma,$  and  $1.3\sigma$  levels respectively. This confirms once again that the constraints on  $\epsilon$  are relatively weak, due to the large uncertainties of the data. We also find that both non- $\Lambda$ CDM cosmological parameters are poorly constrained, with  $w \gtrsim -1.39$  [ $w \gtrsim -1.89$ ] and  $\Omega_K \gtrsim 0.02$  [ $\Omega_K \gtrsim -0.17$ ] at 68% C.L. [95% C.L.], and posterior probabilities  $p(w > -1) = 0.44$  and  $p(\Omega_K > 0) = 0.70$ . All of these figures show no indication for deviations from  $\Lambda$ CDM.

For the FRESCO dataset, we once again find much stronger constraints on  $\epsilon$ , with  $\epsilon \gtrsim 0.53$  and  $\epsilon \gtrsim 0.27$  at 68% and 95% C.L. respectively. Similarly, the data disagrees with our benchmark values  $\epsilon_0 = 0.2, 0.15,$  and  $0.1$  at the  $2.0\sigma, 2.8\sigma,$  and  $3.6\sigma$  levels respectively. This is clearly an improvement over the earlier extensions of  $\Lambda$ CDM, where  $\epsilon_0 = 0.1$  was always disfavored at a significance  $> 5\sigma$ . Nevertheless, our results still indicate that even in this rather general scenario the requirement for high star formation efficiency persists. On the other

hand, the non- $\Lambda$ CDM cosmological parameters remain rather weakly constrained, with  $w \gtrsim -1.38$  [ $w \gtrsim -1.89$ ] and  $\Omega_K \gtrsim 0.09$  [ $\Omega_K \gtrsim -0.11$ ] at 68% C.L. [95% C.L.]. We find no statistically significant indications for deviations from a cosmological constant and/or spatial flatness, with posterior probabilities  $p(w > -1) = 0.48$  and  $p(\Omega_K > 0) = 0.84$ , confirming all earlier results.

The degeneracies between  $\epsilon$ ,  $w$ , and  $\Omega_K$  observed and discussed earlier persist here, although at a weaker level, since they are now redistributed across the parameters: in particular, we still find that  $\epsilon$  is negatively correlated with both  $w$  and  $\Omega_K$ . However, even when moving away from the cosmological constant and allowing for non-zero spatial curvature, FRESCO data continues to require high values of  $\epsilon$ , and show no statistically significant indications for departures from the  $\Lambda$ CDM model.

## 5. DISCUSSION

Our main results are visually summarized in the radar plots of Fig. 6. There we show the Gaussian-equivalent one-sided significance at which values of the baryon-to-star conversion efficiency  $\epsilon < 0.2$  are excluded (left), and 95% one-sided lower limits on  $\epsilon$ , for various different choices of galaxy sample and cosmological model (right). Across all cosmological models considered earlier, we find that photometric data from CEERS provides weak constraints on the baryon-to-star conversion efficiency, albeit hinting at values somewhat larger than those typically assumed in astrophysical contexts, consistently with the earlier results of Boylan-Kolchin (2023). This weak hint is dramatically confirmed by the FRESCO spectroscopic dataset, which robustly requires  $\epsilon \gtrsim 0.3$ – $0.5$  across all cosmological models. All the extensions to  $\Lambda$ CDM we consider relax our constraints but do not qualitatively alter them. Moreover, we find no evidence of deviations from a cosmological constant and spatial flatness. We therefore conclude that, once cosmological uncertainties are marginalized over, cumulative comoving stellar mass density measurements at high redshifts primarily constrain  $\epsilon$ , and show no indication for departures from the flat  $\Lambda$ CDM model. While we have explicitly tested this for a limited set of representative models, our expectation is that this conclusion should hold more generally for cosmological models that smoothly modify the expansion history relative to  $\Lambda$ CDM.

Let us return to one of the key questions raised by early JWST observations, i.e. whether the abundance of massive galaxies at  $z \gtrsim 8$  signals a breakdown of  $\Lambda$ CDM or instead points to more efficient early galaxy and/or star formation (Labbé et al. 2023; Xiao et al. 2024). Our results provide a clear answer: within the class of models we have considered, which are arguably among

the simplest and best motivated extensions to  $\Lambda$ CDM, modifying the background expansion history, and with it the growth of structure, is not sufficient to account for the observed abundances. As discussed earlier, cosmology affects the cumulative stellar mass density primarily through the growth of structure, and in particular through the ratio  $D(z)/D(0)$  when comparing models at fixed  $\sigma_8$ . However, as is clear from Fig. 1, even allowing for very generous variations in  $w$  and  $\Omega_K$ , the resulting changes in the growth factor at the redshifts of interest are typically at the level of tens of percent at best. On the other hand, the values of  $\epsilon$  required by the FRESCO dataset correspond to nearly order unity shifts relative to standard astrophysical expectations. This mismatch in scales implies that generous yet reasonable modifications of the expansion history cannot bridge this gap: *the origin of the “JWST tension” is very unlikely to be cosmological in nature, and should instead be sought in the astrophysics of galaxy formation.*

Our results can be critically compared to earlier works based on the same galaxy samples, most notably those of Boylan-Kolchin (2023) and Xiao et al. (2024) for the CEERS and FRESCO samples respectively. These works already highlighted the potential tension with  $\Lambda$ CDM, but their analyses on the cosmological side were based on a direct comparison between observed and theoretically allowed cumulative stellar mass densities for fixed cosmological and astrophysical parameters, effectively implementing a binary consistency test. We have instead adopted a fully Bayesian approach, which allowed us to simultaneously vary cosmological and astrophysical parameters, while consistently accounting for and propagating uncertainties. As expected, this leads to overall weaker limits on  $\epsilon$ , which nevertheless remain consistent with previous findings. Importantly, we have explicitly demonstrated that the earlier results are largely robust against marginalization over cosmological parameters, and are therefore not driven by assumptions on the underlying cosmological model.

While our results clearly indicate that the observed tension is astrophysical rather than cosmological in nature, the astrophysical interpretation of our findings remains open. Given the cosmological focus of this work, we refrain from detailed speculation on the mechanisms which could lead to the large values of  $\epsilon$  implied by our results. Nevertheless, it is useful to briefly discuss possible effects going in the required direction. The values  $\epsilon \approx 0.7$  implied by the FRESCO dataset are significantly higher than typical expectations from empirical stellar-to-halo mass relations, and may reflect residual systematic uncertainties in the inferred stellar masses and/or number densities. On the observational side,

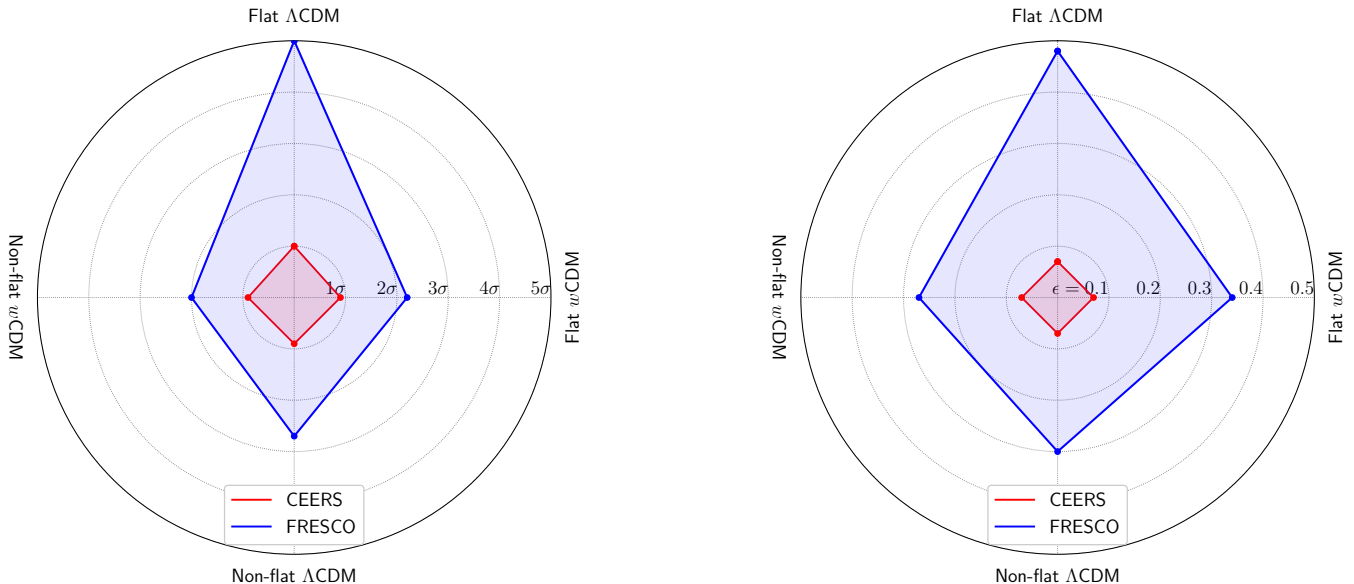


**Figure 6.** Radar plots summarizing our main results, with each spoke corresponding to one of the four cosmological models studied. *Left panel:* radar plot showing the Gaussian-equivalent one-sided significance at which values of the baryon-to-star conversion efficiency  $\epsilon < 0.2$  are excluded in light of the photometric CEERS (red) and spectroscopic FRESKO (blue) samples. *Right panel:* radar plot showing the 95% one-sided lower limits on  $\epsilon$  for the same samples.

systematic uncertainties in stellar mass estimates are known to arise, for instance, from assumptions about the initial mass function (IMF), dust attenuation, and star formation histories, all of which could plausibly bias the inferred masses high. As is clear from Fig. 1, our systems all lie on the steep, exponential decline of the high-mass end of the stellar mass function. Therefore, even rather modest systematic shifts can have a very significant impact on the required values of  $\epsilon$ . On the same token, lensing magnification may also play a role in enhancing the apparent abundance of massive systems. Moreover, we note that most of the UV luminosity is contributed by massive stars. Therefore, a top-heavy IMF of Population-III stars is expected to reduce the required star formation efficiency (see for instance Wang et al. 2023; Hutter et al. 2025; Ziegler et al. 2025). Finally, the inferred cumulative stellar mass densities may also be affected by the limited size of the current galaxy samples. On the theoretical side, additional uncertainties arise from the calibration of the halo mass function at very high redshift. Existing fitting functions are calibrated on numerical simulations over a limited range of masses and redshifts, and are extrapolated in the regime relevant for JWST observations (Reed et al. 2007; Tinker et al. 2008; Watson et al. 2013). Moreover, additional uncertainties can arise from baryonic processes which are yet to be fully understood (Cui et al. 2012; Bocquet et al. 2016; McCarthy et al. 2017). Improved calibration of the high-redshift HMF, informed by ded-

icated simulations, will thus be a crucial step towards assessing the robustness of our results.

Our findings indicate that resolving the “JWST tension” will ultimately require improvements on both the data and modelling sides. On the data side, larger spectroscopic samples will help reduce statistical uncertainties and confirm the nature of the most massive high-redshift systems, thanks to their more robust redshift and stellar mass determinations. At the same time, deep JWST photometry can enable more reliable SED fits which, when combined with spectroscopic information, can help break degeneracies with stellar ages and star-formation history, reducing systematic uncertainties in stellar mass estimates (Luberto et al. 2025). On the theory side, a key role will be played by progress in the calibration of the high-redshift HMF. Advances on these and related points will help determine whether the origin of the “JWST tension” is astrophysical, or lies in new fundamental physics (see also Mehta & Mukherjee 2026, for a recent discussion on how to distinguish between these two scenarios).

## 6. CONCLUSIONS

We have revisited the issue of whether the unexpectedly high abundance of massive, high-redshift galaxies observed by JWST requires new physics beyond  $\Lambda$ CDM, or calls for more astrophysical explanations. Our analysis goes beyond earlier works in three respects. Firstly, while building upon the same “baryon availability” argument adopted earlier (Boylan-Kolchin (2023); Xiao et al.

(2024), we recast the problem using a full likelihood-based analysis which consistently accounts for the fiducial cosmology dependence of the inferred cumulative stellar mass density and stellar masses: this improves over the (simple but conservative) direct comparison, binary consistency test approach adopted earlier, allowing us to consistently propagate uncertainties and ultimately derive a full probability distribution for the baryon-to-star conversion efficiency  $\epsilon$ . Next, to improve the robustness of our results we consider not only the most extreme galaxies within the (photometric) CEERS sample (which provided the first indications of a possible tension with  $\Lambda$ CDM), but also those within the spectroscopic FRESCO sample. Last but not least, we go beyond the  $\Lambda$ CDM model and consider some of its simplest extensions which relax assumptions about the dark energy component and spatial curvature, to assess whether the requirement for high values of  $\epsilon$  can be relaxed going beyond  $\Lambda$ CDM. In short, our work moves beyond earlier fixed cosmological assumptions and per-object minimum-efficiency arguments, performing a full Bayesian analysis of the most extreme galaxies within the CEERS and FRESCO samples. We stress that our goal is not to rule out  $\Lambda$ CDM, but rather to quantify in a fully probabilistic framework what is the range of baryon-to-star conversion efficiencies required once cosmological uncertainties are consistently accounted for.

Our key results are summarized in Fig. 6, and are in qualitative agreement with the earlier findings of [Boylan-Kolchin \(2023\)](#) and [Xiao et al. \(2024\)](#), while being placed on a more robust statistical footing. In a broad brush, we find that the CEERS photometric sample actually leads to comparatively weak constraints on  $\epsilon$ : while there is a mild preference for an enhanced formation efficiency of massive stars, lower values ( $\epsilon \approx 0.1$ ) in agreement with astrophysical expectations are perfectly allowed at 95% C.L., because of the comparatively large uncertainties. Importantly, this picture does not change significantly when moving beyond the flat  $\Lambda$ CDM model. On the other hand, the constraints we derive from FRESCO spectroscopic data are much tighter within all cosmological models, indicating  $\epsilon \gtrsim 0.3 - 0.5$  at 95% C.L., with values  $\epsilon < 0.2$  ruled out at no less than  $2\sigma$ . We obtain especially tight limits within  $\Lambda$ CDM, where we find  $\epsilon \gtrsim 0.48$  at 95% C.L., whereas values  $\epsilon < 0.2$  are ruled out at  $> 5\sigma$ . While moving beyond  $\Lambda$ CDM somewhat relaxes these figures, the need for large values of  $\epsilon$  is only softened but not removed. At the same time, there is no evidence for new physics, as both the dark energy equation of state  $w$  and the spatial curvature parameter  $\Omega_K$  remain consistent with  $-1$  and  $0$  respectively. Our main finding can

therefore be summarized as follows: *the origin of the “JWST tension” is very unlikely to be cosmological in nature, and should instead be sought in the astrophysics of galaxy formation.*

The astrophysical implications of our findings remain open, and we have refrained from speculating on possible effects which could lead to the large values of  $\epsilon$  implied by our results (although we note that our limits assume that the IMF of high-redshift, massive stars is similar to the present-day IMF). Nevertheless, we can confidently state that determining the origin of the “JWST tension” will require improvements on both the data and modelling sides, with larger spectroscopic samples and deeper photometry playing an important role in the former case. On the theory side, we anticipate that it could be interesting to explore additional scenarios, including for instance a (astrophysically well-motivated) redshift- and/or mass-dependent efficiency  $\epsilon(M_{\text{halo}}, z)$ , or looking at the impact of mass functions beyond the Sheth-Tormen one. It is in fact worth recalling that our framework extrapolates at very high redshifts a model which is only well tested at much lower redshifts. While on the cosmology side we have only considered models directly altering the expansion history, and with it the growth of structure, it could be interesting to go beyond this class of models and consider those where the properties of primordial fluctuations are altered, including e.g. models featuring non-Gaussianities or modifications to the primordial power spectrum, all of which could arise from non-standard models of cosmic inflation. At the same time, it is unlikely that models which only directly alter the expansion history, including e.g. those hinted to by the recent DESI observations (see for example [Colgáin et al. 2026](#); [Carloni et al. 2025](#); [Giarè et al. 2024b](#); [Wang & Piao 2026](#); [Yang et al. 2024](#); [Li et al. 2024](#); [Giarè et al. 2024a](#); [Jiang et al. 2024](#); [Giarè 2025](#); [Giarè et al. 2025](#); [Scherer et al. 2025](#); [Chaudhary et al. 2025](#); [Zhang et al. 2025](#); [Li et al. 2026](#); [Capozziello et al. 2026](#)), may loosen the high efficiency requirement while remaining consistent with high-redshift cosmological observations (for the difficulties in this sense, see for instance [Chakraborty et al. 2025](#)). Nevertheless, this point remains to be fully explored.

In closing we note that, for the sake of clarity, we have focused our analysis on the CEERS and FRESCO samples from JWST, which are among the best-studied high-redshift galaxy datasets currently available. It will of course be interesting to extend this work to data from additional JWST programs, especially spectroscopic ones, as well as individual objects that have attracted significant attention in the literature. An example in this sense could be the red, dust-rich galaxy

EGS-Z11-R0 (Rodighiero et al. 2026), although a preliminary assessment shows that its properties are not sufficiently extreme to be in tension with  $\Lambda$ CDM. We leave a full study of these points, and those mentioned earlier, to future work.

#### ACKNOWLEDGEMENTS

We thank Mike Boylan-Kolchin, Ivo Labbé, and Nicola Menci for various very useful discussions, and Steve Murray for promptly fixing an important bug in `hmf` which we identified while this work was being completed. S.V. acknowledges support from the University of Trento and the Provincia Autonoma di Trento (PAT, Autonomous Province of Trento) through the UniTrento Internal Call for Research 2023 grant “Searching for

Dark Energy off the beaten track” (DARKTRACK, grant agreement no. E63C22000500003), and from the Istituto Nazionale di Fisica Nucleare (INFN) through the Commissione Scientifica Nazionale 4 (CSN4) Iniziativa Specifica “Quantum Fields in Gravity, Cosmology and Black Holes” (FLAG). A.L. is partially supported by the Black Hole Initiative at Harvard University, which is funded by grants from the John Templeton Foundation and the Gordon and Betty Moore Foundation. This publication is based upon work from the COST Action CA21136 “Addressing observational tensions in cosmology with systematics and fundamental physics” (CosmoVerse), supported by COST (European Cooperation in Science and Technology).

#### REFERENCES

- Abbott, T. M. C., et al. 2024, *Astrophys. J. Lett.*, 973, L14, doi: [10.3847/2041-8213/ad6ff9](https://doi.org/10.3847/2041-8213/ad6ff9)
- Abdul Karim, M., et al. 2025, *Phys. Rev. D*, 112, 083515, doi: [10.1103/tr6y-kpc6](https://doi.org/10.1103/tr6y-kpc6)
- Adame, A. G., et al. 2025, *JCAP*, 02, 021, doi: [10.1088/1475-7516/2025/02/021](https://doi.org/10.1088/1475-7516/2025/02/021)
- Adil, S. A., Mukhopadhyay, U., Sen, A. A., & Vagnozzi, S. 2023, *JCAP*, 10, 072, doi: [10.1088/1475-7516/2023/10/072](https://doi.org/10.1088/1475-7516/2023/10/072)
- Aghanim, N., et al. 2020, *Astron. Astrophys.*, 641, A6, doi: [10.1051/0004-6361/201833910](https://doi.org/10.1051/0004-6361/201833910)
- Akarsu, Ö., Colgáin, E. Ó., Sen, A. A., & Sheikh-Jabbari, M. M. 2024, *Universe*, 10, 305, doi: [10.3390/universe10080305](https://doi.org/10.3390/universe10080305)
- Akarsu, O., Di Valentino, E., Kumar, S., Ozyigit, M., & Sharma, S. 2023, *Phys. Dark Univ.*, 39, 101162, doi: [10.1016/j.dark.2022.101162](https://doi.org/10.1016/j.dark.2022.101162)
- Bargiacchi, G., Benetti, M., Capozziello, S., et al. 2022, *Mon. Not. Roy. Astron. Soc.*, 515, 1795, doi: [10.1093/mnras/stac1941](https://doi.org/10.1093/mnras/stac1941)
- Baryakhtar, M., Simon, O., & Weiner, Z. J. 2024, *Phys. Rev. D*, 110, 083505, doi: [10.1103/PhysRevD.110.083505](https://doi.org/10.1103/PhysRevD.110.083505)
- Behroozi, P. S., Wechsler, R. H., & Conroy, C. 2013a, *Astrophys. J.*, 770, 57, doi: [10.1088/0004-637X/770/1/57](https://doi.org/10.1088/0004-637X/770/1/57)
- . 2013b, *Astrophys. J. Lett.*, 762, L31, doi: [10.1088/2041-8205/762/2/L31](https://doi.org/10.1088/2041-8205/762/2/L31)
- Bel, J., Larena, J., Maartens, R., Marinoni, C., & Perenon, L. 2022, *JCAP*, 09, 076, doi: [10.1088/1475-7516/2022/09/076](https://doi.org/10.1088/1475-7516/2022/09/076)
- Benisty, D., & Staicova, D. 2021, *Astron. Astrophys.*, 647, A38, doi: [10.1051/0004-6361/202039502](https://doi.org/10.1051/0004-6361/202039502)
- Biagetti, M., Franciolini, G., & Riotto, A. 2023, *Astrophys. J.*, 944, 113, doi: [10.3847/1538-4357/acb5ea](https://doi.org/10.3847/1538-4357/acb5ea)
- Bigiel, F., Leroy, A., Walter, F., et al. 2008, *Astron. J.*, 136, 2846, doi: [10.1088/0004-6256/136/6/2846](https://doi.org/10.1088/0004-6256/136/6/2846)
- Binici, S. S., Deliduman, C., & Dilsiz, F. Ş. 2024, *Phys. Dark Univ.*, 46, 101600, doi: [10.1016/j.dark.2024.101600](https://doi.org/10.1016/j.dark.2024.101600)
- Bird, S., Chang, C.-F., Cui, Y., & Yang, D. 2024, *Phys. Lett. B*, 858, 139062, doi: [10.1016/j.physletb.2024.139062](https://doi.org/10.1016/j.physletb.2024.139062)
- Bocquet, S., Saro, A., Dolag, K., & Mohr, J. J. 2016, *Mon. Not. Roy. Astron. Soc.*, 456, 2361, doi: [10.1093/mnras/stv2657](https://doi.org/10.1093/mnras/stv2657)
- Boylan-Kolchin, M. 2023, *Nature Astron.*, 7, 731, doi: [10.1038/s41550-023-01937-7](https://doi.org/10.1038/s41550-023-01937-7)
- . 2025, *Mon. Not. Roy. Astron. Soc.*, 538, 3210, doi: [10.1093/mnras/staf471](https://doi.org/10.1093/mnras/staf471)
- Cao, S., Ryan, J., & Ratra, B. 2021, *Mon. Not. Roy. Astron. Soc.*, 504, 300, doi: [10.1093/mnras/stab942](https://doi.org/10.1093/mnras/stab942)
- Capozziello, S., Chaudhary, H., Harko, T., & Mustafa, G. 2026, *Phys. Dark Univ.*, 51, 102196, doi: [10.1016/j.dark.2025.102196](https://doi.org/10.1016/j.dark.2025.102196)
- Carlóni, Y., Luongo, O., & Muccino, M. 2025, *Phys. Rev. D*, 111, 023512, doi: [10.1103/PhysRevD.111.023512](https://doi.org/10.1103/PhysRevD.111.023512)
- Casey, C. M., et al. 2024, *Astrophys. J.*, 965, 98, doi: [10.3847/1538-4357/ad2075](https://doi.org/10.3847/1538-4357/ad2075)
- Chakraborty, A., Choudhury, T. R., Sen, A. A., & Mukherjee, P. 2025, doi: [10.1093/mnras/stag269](https://doi.org/10.1093/mnras/stag269)
- Chaudhary, H., Capozziello, S., Sharma, V. K., & Mustafa, G. 2025, *Astrophys. J.*, 992, 194, doi: [10.3847/1538-4357/ae0458](https://doi.org/10.3847/1538-4357/ae0458)
- Chudaykin, A., Dolgikh, K., & Ivanov, M. M. 2021, *Phys. Rev. D*, 103, 023507, doi: [10.1103/PhysRevD.103.023507](https://doi.org/10.1103/PhysRevD.103.023507)
- Chudaykin, A., Ivanov, M. M., & Philcox, O. H. E. 2026, *Phys. Rev. D*, 113, 063502, doi: [10.1103/qsnt-dppc](https://doi.org/10.1103/qsnt-dppc)
- Colgáin, E. Ó., Dainotti, M. G., Capozziello, S., et al. 2026, *JHEAp*, 49, 100428, doi: [10.1016/j.jheap.2025.100428](https://doi.org/10.1016/j.jheap.2025.100428)

- Colgáin, E. Ó., Pourojaghi, S., & Sheikh-Jabbari, M. M. 2025a, *Eur. Phys. J. C*, 85, 286, doi: [10.1140/epjc/s10052-025-13995-4](https://doi.org/10.1140/epjc/s10052-025-13995-4)
- Colgáin, E. Ó., & Sheikh-Jabbari, M. M. 2025, *Mon. Not. Roy. Astron. Soc.*, 542, L24, doi: [10.1093/mnras/slaf042](https://doi.org/10.1093/mnras/slaf042)
- Colgáin, E. Ó., Sheikh-Jabbari, M. M., & Yin, L. 2025b, *Phys. Dark Univ.*, 49, 101975, doi: [10.1016/j.dark.2025.101975](https://doi.org/10.1016/j.dark.2025.101975)
- Conroy, C., & Wechsler, R. H. 2009, *Astrophys. J.*, 696, 620, doi: [10.1088/0004-637X/696/1/620](https://doi.org/10.1088/0004-637X/696/1/620)
- Costa, A. A., Ren, Z., & Yin, Z. 2023, *Eur. Phys. J. C*, 83, 875, doi: [10.1140/epjc/s10052-023-12038-0](https://doi.org/10.1140/epjc/s10052-023-12038-0)
- Cui, W., Borgani, S., Dolag, K., Murante, G., & Tornatore, L. 2012, *Mon. Not. Roy. Astron. Soc.*, 423, 2279, doi: [10.1111/j.1365-2966.2012.21037.x](https://doi.org/10.1111/j.1365-2966.2012.21037.x)
- Das, S., Mondol, R., Singh, A., & Laha, R. 2025, <https://arxiv.org/abs/2511.02906>
- Dayal, P., & Giri, S. K. 2024, *Mon. Not. Roy. Astron. Soc.*, 528, 2784, doi: [10.1093/mnras/stae176](https://doi.org/10.1093/mnras/stae176)
- Dekel, A., Sarkar, K. C., Birnboim, Y., Mandelker, N., & Li, Z. 2023, *Mon. Not. Roy. Astron. Soc.*, 523, 3201, doi: [10.1093/mnras/stad1557](https://doi.org/10.1093/mnras/stad1557)
- Dhawan, S., Alsing, J., & Vagnozzi, S. 2021, *Mon. Not. Roy. Astron. Soc.*, 506, L1, doi: [10.1093/mnras/slab058](https://doi.org/10.1093/mnras/slab058)
- Di Valentino, E., Melchiorri, A., Mena, O., Pan, S., & Yang, W. 2021a, *Mon. Not. Roy. Astron. Soc.*, 502, L23, doi: [10.1093/mnras/slaa207](https://doi.org/10.1093/mnras/slaa207)
- Di Valentino, E., Melchiorri, A., & Silk, J. 2019, *Nature Astron.*, 4, 196, doi: [10.1038/s41550-019-0906-9](https://doi.org/10.1038/s41550-019-0906-9)
- . 2021b, *Astrophys. J. Lett.*, 908, L9, doi: [10.3847/2041-8213/ab1c4](https://doi.org/10.3847/2041-8213/ab1c4)
- Di Valentino, E., et al. 2025, *Phys. Dark Univ.*, 49, 101965, doi: [10.1016/j.dark.2025.101965](https://doi.org/10.1016/j.dark.2025.101965)
- Dinda, B. R. 2022, *Phys. Rev. D*, 105, 063524, doi: [10.1103/PhysRevD.105.063524](https://doi.org/10.1103/PhysRevD.105.063524)
- Du, G.-H., Wu, P.-J., Li, T.-N., & Zhang, X. 2025, *Eur. Phys. J. C*, 85, 392, doi: [10.1140/epjc/s10052-025-14094-0](https://doi.org/10.1140/epjc/s10052-025-14094-0)
- Efstathiou, G., & Gratton, S. 2020, *Mon. Not. Roy. Astron. Soc.*, 496, L91, doi: [10.1093/mnras/slao093](https://doi.org/10.1093/mnras/slao093)
- Escamilla, L. A., Giarè, W., Di Valentino, E., Nunes, R. C., & Vagnozzi, S. 2024, *JCAP*, 05, 091, doi: [10.1088/1475-7516/2024/05/091](https://doi.org/10.1088/1475-7516/2024/05/091)
- Fakhry, S., Salmani, R. V., & Firouzjaee, J. T. 2025, *Phys. Rev. D*, 112, 123503, doi: [10.1103/9cmb-kf3x](https://doi.org/10.1103/9cmb-kf3x)
- Fakhry, S., Shiravand, M., & Del Popolo, A. 2026, *Astrophys. J.*, 998, 178, doi: [10.3847/1538-4357/ae371b](https://doi.org/10.3847/1538-4357/ae371b)
- Favale, A., Gómez-Valent, A., & Migliaccio, M. 2023, *Mon. Not. Roy. Astron. Soc.*, 523, 3406, doi: [10.1093/mnras/stad1621](https://doi.org/10.1093/mnras/stad1621)
- Feng, L., Li, T.-N., Du, G.-H., Zhang, J.-F., & Zhang, X. 2026, *Phys. Dark Univ.*, 52, 102296, doi: [10.1016/j.dark.2026.102296](https://doi.org/10.1016/j.dark.2026.102296)
- Ferrara, A., Pallottini, A., & Dayal, P. 2023, *Mon. Not. Roy. Astron. Soc.*, 522, 3986, doi: [10.1093/mnras/stad1095](https://doi.org/10.1093/mnras/stad1095)
- Forconi, M., & Di Valentino, E. 2025, *Phys. Dark Univ.*, 48, 101904, doi: [10.1016/j.dark.2025.101904](https://doi.org/10.1016/j.dark.2025.101904)
- Forconi, M., Giarè, W., Mena, O., et al. 2024, *JCAP*, 05, 097, doi: [10.1088/1475-7516/2024/05/097](https://doi.org/10.1088/1475-7516/2024/05/097)
- Forconi, M., Ruchika, Melchiorri, A., Mena, O., & Menci, N. 2023, *JCAP*, 10, 012, doi: [10.1088/1475-7516/2023/10/012](https://doi.org/10.1088/1475-7516/2023/10/012)
- Foreman-Mackey, D., Hogg, D. W., Lang, D., & Goodman, J. 2013, *Publ. Astron. Soc. Pac.*, 125, 306, doi: [10.1086/670067](https://doi.org/10.1086/670067)
- Gandolfi, G., Lapi, A., Ronconi, T., & Danese, L. 2022, *Universe*, 8, 589, doi: [10.3390/universe8110589](https://doi.org/10.3390/universe8110589)
- Gardner, J. P., et al. 2006, *Space Sci. Rev.*, 123, 485, doi: [10.1007/s11214-006-8315-7](https://doi.org/10.1007/s11214-006-8315-7)
- Giarè, W. 2025, *Phys. Rev. D*, 112, 023508, doi: [10.1103/ss37-cxhn](https://doi.org/10.1103/ss37-cxhn)
- Giarè, W., Di Valentino, E., & Melchiorri, A. 2024, *Phys. Rev. D*, 109, 103519, doi: [10.1103/PhysRevD.109.103519](https://doi.org/10.1103/PhysRevD.109.103519)
- Giarè, W., Mahassen, T., Di Valentino, E., & Pan, S. 2025, *Phys. Dark Univ.*, 48, 101906, doi: [10.1016/j.dark.2025.101906](https://doi.org/10.1016/j.dark.2025.101906)
- Giarè, W., Najafi, M., Pan, S., Di Valentino, E., & Firouzjaee, J. T. 2024a, *JCAP*, 10, 035, doi: [10.1088/1475-7516/2024/10/035](https://doi.org/10.1088/1475-7516/2024/10/035)
- Giarè, W., Sabogal, M. A., Nunes, R. C., & Di Valentino, E. 2024b, *Phys. Rev. Lett.*, 133, 251003, doi: [10.1103/PhysRevLett.133.251003](https://doi.org/10.1103/PhysRevLett.133.251003)
- Glanville, A., Howlett, C., & Davis, T. M. 2022, *Mon. Not. Roy. Astron. Soc.*, 517, 3087, doi: [10.1093/mnras/stac2891](https://doi.org/10.1093/mnras/stac2891)
- Gonzalez, J. E., Benetti, M., von Marttens, R., & Alcaniz, J. 2021, *JCAP*, 11, 060, doi: [10.1088/1475-7516/2021/11/060](https://doi.org/10.1088/1475-7516/2021/11/060)
- Green, D., & Meyers, J. 2025, *Phys. Rev. D*, 111, 083507, doi: [10.1103/PhysRevD.111.083507](https://doi.org/10.1103/PhysRevD.111.083507)
- Guo, S.-Y., Khlopov, M., Liu, X., et al. 2024, *Sci. China Phys. Mech. Astron.*, 67, 111011, doi: [10.1007/s11433-024-2445-1](https://doi.org/10.1007/s11433-024-2445-1)
- Gupta, R. P. 2023, *Mon. Not. Roy. Astron. Soc.*, 524, 3385, doi: [10.1093/mnras/stad2032](https://doi.org/10.1093/mnras/stad2032)
- Handley, W. 2021, *Phys. Rev. D*, 103, L041301, doi: [10.1103/PhysRevD.103.L041301](https://doi.org/10.1103/PhysRevD.103.L041301)

- Haslbauer, M., Kroupa, P., Zonoozi, A. H., & Haggi, H. 2022, *Astrophys. J. Lett.*, 939, L31, doi: [10.3847/2041-8213/ac9a50](https://doi.org/10.3847/2041-8213/ac9a50)
- Hegde, S., Wyatt, M. M., & Furlanetto, S. R. 2024, *JCAP*, 08, 025, doi: [10.1088/1475-7516/2024/08/025](https://doi.org/10.1088/1475-7516/2024/08/025)
- Huang, H.-L., Cai, Y., Jiang, J.-Q., Zhang, J., & Piao, Y.-S. 2024a, *Res. Astron. Astrophys.*, 24, 091001, doi: [10.1088/1674-4527/ad683d](https://doi.org/10.1088/1674-4527/ad683d)
- Huang, H.-L., Jiang, J.-Q., & Piao, Y.-S. 2024b, *Phys. Rev. D*, 110, 103540, doi: [10.1103/PhysRevD.110.103540](https://doi.org/10.1103/PhysRevD.110.103540)
- Hütsi, G., Raidal, M., Urrutia, J., Vaskonen, V., & Veermäe, H. 2023, *Phys. Rev. D*, 107, 043502, doi: [10.1103/PhysRevD.107.043502](https://doi.org/10.1103/PhysRevD.107.043502)
- Hutter, A., Cueto, E. R., Dayal, P., et al. 2025, *Astron. Astrophys.*, 694, A254, doi: [10.1051/0004-6361/202452460](https://doi.org/10.1051/0004-6361/202452460)
- Ilie, C., Paulin, J., & Freese, K. 2023, *Proc. Nat. Acad. Sci.*, 120, e2305762120, doi: [10.1073/pnas.2305762120](https://doi.org/10.1073/pnas.2305762120)
- Iocco, F., & Visinelli, L. 2024, *Phys. Dark Univ.*, 44, 101496, doi: [10.1016/j.dark.2024.101496](https://doi.org/10.1016/j.dark.2024.101496)
- Jiang, J.-Q., Liu, W., Zhan, H., & Hu, B. 2025a, *Phys. Rev. D*, 111, 023519, doi: [10.1103/PhysRevD.111.023519](https://doi.org/10.1103/PhysRevD.111.023519)
- Jiang, J.-Q., Pedrotti, D., da Costa, S. S., & Vagnozzi, S. 2024, *Phys. Rev. D*, 110, 123519, doi: [10.1103/PhysRevD.110.123519](https://doi.org/10.1103/PhysRevD.110.123519)
- Jiang, J.-Q., Giarè, W., Gariazzo, S., et al. 2025b, *JCAP*, 01, 153, doi: [10.1088/1475-7516/2025/01/153](https://doi.org/10.1088/1475-7516/2025/01/153)
- Jiao, H., Brandenberger, R., & Refregier, A. 2023, *Phys. Rev. D*, 108, 043510, doi: [10.1103/PhysRevD.108.043510](https://doi.org/10.1103/PhysRevD.108.043510)
- Kennicutt, Jr., R. C., & Evans, II, N. J. 2012, *Ann. Rev. Astron. Astrophys.*, 50, 531, doi: [10.1146/annurev-astro-081811-125610](https://doi.org/10.1146/annurev-astro-081811-125610)
- Labbé, I., et al. 2023, *Nature*, 616, 266, doi: [10.1038/s41586-023-05786-2](https://doi.org/10.1038/s41586-023-05786-2)
- Lee, S. 2025, *Mon. Not. Roy. Astron. Soc.*, 544, 3388, doi: [10.1093/mnras/staf1890](https://doi.org/10.1093/mnras/staf1890)
- . 2026, *Eur. Phys. J. C*, 86, 297, doi: [10.1140/epjc/s10052-026-15541-2](https://doi.org/10.1140/epjc/s10052-026-15541-2)
- Lei, L., Wang, Y.-Y., Yuan, G.-W., et al. 2025, *Astrophys. J.*, 980, 249, doi: [10.3847/1538-4357/ada93b](https://doi.org/10.3847/1538-4357/ada93b)
- Lei, L., Wang, Z.-F., Wang, T.-L., et al. 2026, *Mon. Not. Roy. Astron. Soc.*, 547, 1, doi: [10.1093/mnras/stag430](https://doi.org/10.1093/mnras/stag430)
- Lei, L., et al. 2024, *Sci. China Phys. Mech. Astron.*, 67, 229811, doi: [10.1007/s11433-023-2233-2](https://doi.org/10.1007/s11433-023-2233-2)
- Leroy, A. K., Walter, F., Brinks, E., et al. 2008, *Astron. J.*, 136, 2782, doi: [10.1088/0004-6256/136/6/2782](https://doi.org/10.1088/0004-6256/136/6/2782)
- Lewis, A. 2025, *JCAP*, 08, 025, doi: [10.1088/1475-7516/2025/08/025](https://doi.org/10.1088/1475-7516/2025/08/025)
- Li, T.-N., Du, G.-H., Zhou, S.-H., et al. 2026, *Phys. Dark Univ.*, 52, 102254, doi: [10.1016/j.dark.2026.102254](https://doi.org/10.1016/j.dark.2026.102254)
- Li, T.-N., Wu, P.-J., Du, G.-H., et al. 2024, *Astrophys. J.*, 976, 1, doi: [10.3847/1538-4357/ad87f0](https://doi.org/10.3847/1538-4357/ad87f0)
- Lin, H., Gong, Y., Yue, B., & Chen, X. 2024, *Res. Astron. Astrophys.*, 24, 015009, doi: [10.1088/1674-4527/ad0864](https://doi.org/10.1088/1674-4527/ad0864)
- Lin, W., Chen, X., & Mack, K. J. 2021, *Astrophys. J.*, 920, 159, doi: [10.3847/1538-4357/ac12cf](https://doi.org/10.3847/1538-4357/ac12cf)
- Liu, B., & Bromm, V. 2022, *Astrophys. J. Lett.*, 937, L30, doi: [10.3847/2041-8213/ac927f](https://doi.org/10.3847/2041-8213/ac927f)
- Liu, T., Wang, S., Wu, H., Cao, S., & Wang, J. 2025, *Astrophys. J. Lett.*, 981, L24, doi: [10.3847/2041-8213/adb7de](https://doi.org/10.3847/2041-8213/adb7de)
- Loverde, M., & Weiner, Z. J. 2024, *JCAP*, 12, 048, doi: [10.1088/1475-7516/2024/12/048](https://doi.org/10.1088/1475-7516/2024/12/048)
- Lu, S., Frenk, C. S., Bose, S., et al. 2024, *Mon. Not. Roy. Astron. Soc.*, 536, 1018, doi: [10.1093/mnras/stae2646](https://doi.org/10.1093/mnras/stae2646)
- Luberto, J., Furlanetto, S., & Mirocha, J. 2025, *JCAP*, 10, 084, doi: [10.1088/1475-7516/2025/10/084](https://doi.org/10.1088/1475-7516/2025/10/084)
- Luongo, O., & Muccino, M. 2024, *Astron. Astrophys.*, 690, A40, doi: [10.1051/0004-6361/202450512](https://doi.org/10.1051/0004-6361/202450512)
- Lynch, G. P., & Knox, L. 2025, *Phys. Rev. D*, 112, 083543, doi: [10.1103/613p-pph2](https://doi.org/10.1103/613p-pph2)
- Maio, U., & Viel, M. 2023, *Astron. Astrophys.*, 672, A71, doi: [10.1051/0004-6361/202345851](https://doi.org/10.1051/0004-6361/202345851)
- McCarthy, I. G., Schaye, J., Bird, S., & Le Brun, A. M. C. 2017, *Mon. Not. Roy. Astron. Soc.*, 465, 2936, doi: [10.1093/mnras/stw2792](https://doi.org/10.1093/mnras/stw2792)
- Mehta, H., & Mukherjee, S. 2026, *Astrophys. J.*, 998, 143, doi: [10.3847/1538-4357/ae3170](https://doi.org/10.3847/1538-4357/ae3170)
- Menci, N., Adil, S. A., Mukhopadhyay, U., Sen, A. A., & Vagnozzi, S. 2024a, *JCAP*, 07, 072, doi: [10.1088/1475-7516/2024/07/072](https://doi.org/10.1088/1475-7516/2024/07/072)
- Menci, N., Castellano, M., Mukherjee, P., et al. 2026, *Astron. Astrophys.*, 707, A300, doi: [10.1051/0004-6361/202558610](https://doi.org/10.1051/0004-6361/202558610)
- Menci, N., Castellano, M., Santini, P., et al. 2022, *Astrophys. J. Lett.*, 938, L5, doi: [10.3847/2041-8213/ac96e9](https://doi.org/10.3847/2041-8213/ac96e9)
- Menci, N., Sen, A. A., & Castellano, M. 2024b, *Astrophys. J.*, 976, 227, doi: [10.3847/1538-4357/ad8d5b](https://doi.org/10.3847/1538-4357/ad8d5b)
- Moster, B. P., Naab, T., & White, S. D. M. 2013, *Mon. Not. Roy. Astron. Soc.*, 428, 3121, doi: [10.1093/mnras/sts261](https://doi.org/10.1093/mnras/sts261)
- Murray, S., Power, C., & Robotham, A. S. G. 2013, *Astron. Comput.*, 3-4, 23, doi: [10.1016/j.ascom.2013.11.001](https://doi.org/10.1016/j.ascom.2013.11.001)
- Naredo-Tuero, D., Escudero, M., Fernández-Martínez, E., Marcano, X., & Poulin, V. 2024, *Phys. Rev. D*, 110, 123537, doi: [10.1103/PhysRevD.110.123537](https://doi.org/10.1103/PhysRevD.110.123537)
- Pacucci, F., Nguyen, B., Carniani, S., Maiolino, R., & Fan, X. 2023, *Astrophys. J. Lett.*, 957, L3, doi: [10.3847/2041-8213/ad0158](https://doi.org/10.3847/2041-8213/ad0158)

- Padmanabhan, H., & Loeb, A. 2023, *Astrophys. J. Lett.*, 953, L4, doi: [10.3847/2041-8213/acea7a](https://doi.org/10.3847/2041-8213/acea7a)
- Pallottini, A., & Ferrara, A. 2023, *Astron. Astrophys.*, 677, L4, doi: [10.1051/0004-6361/202347384](https://doi.org/10.1051/0004-6361/202347384)
- Parashari, P., & Laha, R. 2023, *Mon. Not. Roy. Astron. Soc.*, 526, L63, doi: [10.1093/mnras/slad107](https://doi.org/10.1093/mnras/slad107)
- Pedrotti, D., Escamilla, L. A., Marra, V., Perivolaropoulos, L., & Vagnozzi, S. 2026, *Phys. Rev. D*, 113, 043507, doi: [10.1103/pn9j-8whx](https://doi.org/10.1103/pn9j-8whx)
- Pedrotti, D., Jiang, J.-Q., Escamilla, L. A., da Costa, S. S., & Vagnozzi, S. 2025, *Phys. Rev. D*, 111, 023506, doi: [10.1103/PhysRevD.111.023506](https://doi.org/10.1103/PhysRevD.111.023506)
- Qi, J.-Z., Meng, P., Zhang, J.-F., & Zhang, X. 2023, *Phys. Rev. D*, 108, 063522, doi: [10.1103/PhysRevD.108.063522](https://doi.org/10.1103/PhysRevD.108.063522)
- Qin, Y., Balu, S., & Wyithe, J. S. B. 2023, *Mon. Not. Roy. Astron. Soc.*, 526, 1324, doi: [10.1093/mnras/stad2448](https://doi.org/10.1093/mnras/stad2448)
- Reed, D., Bower, R., Frenk, C., Jenkins, A., & Theuns, T. 2007, *Mon. Not. Roy. Astron. Soc.*, 374, 2, doi: [10.1111/j.1365-2966.2006.11204.x](https://doi.org/10.1111/j.1365-2966.2006.11204.x)
- Robitaille, T. P., et al. 2013, *Astron. Astrophys.*, 558, A33, doi: [10.1051/0004-6361/201322068](https://doi.org/10.1051/0004-6361/201322068)
- Rodighiero, G., Ferrara, A., Catone, M., et al. 2026, arXiv e-prints, arXiv:2603.15841, doi: [10.48550/arXiv.2603.15841](https://doi.org/10.48550/arXiv.2603.15841)
- Roy Choudhury, S. 2025, *Astrophys. J. Lett.*, 986, L31, doi: [10.3847/2041-8213/ade1cc](https://doi.org/10.3847/2041-8213/ade1cc)
- Roy Choudhury, S., & Hannestad, S. 2020, *JCAP*, 07, 037, doi: [10.1088/1475-7516/2020/07/037](https://doi.org/10.1088/1475-7516/2020/07/037)
- Roy Choudhury, S., & Naskar, A. 2019, *Eur. Phys. J. C*, 79, 262, doi: [10.1140/epjc/s10052-019-6762-z](https://doi.org/10.1140/epjc/s10052-019-6762-z)
- Roy Choudhury, S., & Okumura, T. 2024, *Astrophys. J. Lett.*, 976, L11, doi: [10.3847/2041-8213/ad8c26](https://doi.org/10.3847/2041-8213/ad8c26)
- Roy Choudhury, S., Okumura, T., & Umetsu, K. 2025, *Astrophys. J. Lett.*, 994, L26, doi: [10.3847/2041-8213/ae1a64](https://doi.org/10.3847/2041-8213/ae1a64)
- Rubin, D., et al. 2025, *Astrophys. J.*, 986, 231, doi: [10.3847/1538-4357/adc0a5](https://doi.org/10.3847/1538-4357/adc0a5)
- Sakr, Z. 2023, *Phys. Rev. D*, 108, 083519, doi: [10.1103/PhysRevD.108.083519](https://doi.org/10.1103/PhysRevD.108.083519)
- Sammur, K. 2025. <https://arxiv.org/abs/2507.11237>
- Scherer, M., Sabogal, M. A., Nunes, R. C., & De Felice, A. 2025, *Phys. Rev. D*, 112, 043513, doi: [10.1103/n86r-sjgm](https://doi.org/10.1103/n86r-sjgm)
- Shen, X., Vogelsberger, M., Boylan-Kolchin, M., Tacchella, S., & Kannan, R. 2023. <https://arxiv.org/abs/2305.05679>
- Shen, X., et al. 2026, *Mon. Not. Roy. Astron. Soc.*, 545, staf2119, doi: [10.1093/mnras/staf2119](https://doi.org/10.1093/mnras/staf2119)
- Sheth, R. K., Mo, H. J., & Tormen, G. 2001, *Mon. Not. Roy. Astron. Soc.*, 323, 1, doi: [10.1046/j.1365-8711.2001.04006.x](https://doi.org/10.1046/j.1365-8711.2001.04006.x)
- Shlivko, D., & Poulin, V. 2026. <https://arxiv.org/abs/2603.22406>
- Shuntov, M., et al. 2022, *Astron. Astrophys.*, 664, A61, doi: [10.1051/0004-6361/202243136](https://doi.org/10.1051/0004-6361/202243136)
- Specogna, E., Vardanyan, T., Giarè, W., & Di Valentino, E. 2025. <https://arxiv.org/abs/2509.26263>
- Stevens, J., Khoraminezhad, H., & Saito, S. 2023, *JCAP*, 07, 046, doi: [10.1088/1475-7516/2023/07/046](https://doi.org/10.1088/1475-7516/2023/07/046)
- Su, B.-Y., Li, N., & Feng, L. 2023. <https://arxiv.org/abs/2306.05364>
- Sun, G., Faucher-Giguère, C.-A., Hayward, C. C., et al. 2023, *Astrophys. J. Lett.*, 955, L35, doi: [10.3847/2041-8213/acf85a](https://doi.org/10.3847/2041-8213/acf85a)
- Tacchella, S., Bose, S., Conroy, C., Eisenstein, D. J., & Johnson, B. D. 2018, *Astrophys. J.*, 868, 92, doi: [10.3847/1538-4357/aae8e0](https://doi.org/10.3847/1538-4357/aae8e0)
- Tanseri, I., Hagstotz, S., Vagnozzi, S., Giusarma, E., & Freese, K. 2022, *JHEAp*, 36, 1, doi: [10.1016/j.jheap.2022.07.002](https://doi.org/10.1016/j.jheap.2022.07.002)
- Tinker, J. L., Kravtsov, A. V., Klypin, A., et al. 2008, *Astrophys. J.*, 688, 709, doi: [10.1086/591439](https://doi.org/10.1086/591439)
- Vagnozzi, S. 2020, *Phys. Rev. D*, 102, 023518, doi: [10.1103/PhysRevD.102.023518](https://doi.org/10.1103/PhysRevD.102.023518)
- Vagnozzi, S., Dhawan, S., Gerbino, M., et al. 2018, *Phys. Rev. D*, 98, 083501, doi: [10.1103/PhysRevD.98.083501](https://doi.org/10.1103/PhysRevD.98.083501)
- Vagnozzi, S., Di Valentino, E., Gariazzo, S., et al. 2021a, *Phys. Dark Univ.*, 33, 100851, doi: [10.1016/j.dark.2021.100851](https://doi.org/10.1016/j.dark.2021.100851)
- Vagnozzi, S., Giusarma, E., Mena, O., et al. 2017, *Phys. Rev. D*, 96, 123503, doi: [10.1103/PhysRevD.96.123503](https://doi.org/10.1103/PhysRevD.96.123503)
- Vagnozzi, S., Loeb, A., & Moresco, M. 2021b, *Astrophys. J.*, 908, 84, doi: [10.3847/1538-4357/abd4df](https://doi.org/10.3847/1538-4357/abd4df)
- Vagnozzi, S., Pacucci, F., & Loeb, A. 2022, *JHEAp*, 36, 27, doi: [10.1016/j.jheap.2022.07.004](https://doi.org/10.1016/j.jheap.2022.07.004)
- van Putten, M. H. P. M. 2024, *Phys. Dark Univ.*, 43, 101417, doi: [10.1016/j.dark.2023.101417](https://doi.org/10.1016/j.dark.2023.101417)
- Wang, B., Qi, J.-Z., Zhang, J.-F., & Zhang, X. 2020, *Astrophys. J.*, 898, 100, doi: [10.3847/1538-4357/ab9b22](https://doi.org/10.3847/1538-4357/ab9b22)
- Wang, D., & Liu, Y. 2022. <https://arxiv.org/abs/2301.00347>
- Wang, D., Mena, O., Di Valentino, E., & Gariazzo, S. 2024a, *Phys. Rev. D*, 110, 103536, doi: [10.1103/PhysRevD.110.103536](https://doi.org/10.1103/PhysRevD.110.103536)
- Wang, H., & Piao, Y.-S. 2026, *Phys. Lett. B*, 873, 140180, doi: [10.1016/j.physletb.2026.140180](https://doi.org/10.1016/j.physletb.2026.140180)
- Wang, J., Huang, Z., Huang, L., & Liu, J. 2024b, *Res. Astron. Astrophys.*, 24, 045001, doi: [10.1088/1674-4527/ad2cd3](https://doi.org/10.1088/1674-4527/ad2cd3)
- Wang, J.-Q., Cai, R.-G., Guo, Z.-K., & Wang, S.-J. 2025. <https://arxiv.org/abs/2508.01759>

- Wang, P., Su, B.-Y., Zu, L., Yang, Y., & Feng, L. 2024c, *Eur. Phys. J. Plus*, 139, 711, doi: [10.1140/epjp/s13360-024-05276-y](https://doi.org/10.1140/epjp/s13360-024-05276-y)
- Wang, Y., & Lin, W. 2025, *Astrophys. J.*, 989, 120, doi: [10.3847/1538-4357/adf336](https://doi.org/10.3847/1538-4357/adf336)
- Wang, Y.-Y., Lei, L., Yuan, G.-W., & Fan, Y.-Z. 2023, *Astrophys. J. Lett.*, 954, L48, doi: [10.3847/2041-8213/acf46c](https://doi.org/10.3847/2041-8213/acf46c)
- Wang, Z.-F., Lei, L., Feng, L., & Fan, Y.-Z. 2024d, *Res. Astron. Astrophys.*, 24, 125012, doi: [10.1088/1674-4527/ad9198](https://doi.org/10.1088/1674-4527/ad9198)
- Watson, W. A., Iliev, I. T., D'Aloisio, A., et al. 2013, *Mon. Not. Roy. Astron. Soc.*, 433, 1230, doi: [10.1093/mnras/stt791](https://doi.org/10.1093/mnras/stt791)
- Wechsler, R. H., & Tinker, J. L. 2018, *Ann. Rev. Astron. Astrophys.*, 56, 435, doi: [10.1146/annurev-astro-081817-051756](https://doi.org/10.1146/annurev-astro-081817-051756)
- Wei, J.-J., & Melia, F. 2022, *Astrophys. J.*, 928, 165, doi: [10.3847/1538-4357/ac562c](https://doi.org/10.3847/1538-4357/ac562c)
- Weiner, Z. J. 2026. <https://arxiv.org/abs/2603.18131>
- Wu, P.-J., Qi, J.-Z., & Zhang, X. 2023, *Chin. Phys. C*, 47, 055106, doi: [10.1088/1674-1137/acc647](https://doi.org/10.1088/1674-1137/acc647)
- Wu, P.-J., & Zhang, X. 2025, *Phys. Rev. D*, 112, 063514, doi: [10.1103/sn3q-q589](https://doi.org/10.1103/sn3q-q589)
- Xiao, M., et al. 2024, *Nature*, 635, 311, doi: [10.1038/s41586-024-08094-5](https://doi.org/10.1038/s41586-024-08094-5)
- Yadav, M., Dixit, A., Barak, M. S., & Pradhan, A. 2025, *Eur. Phys. J. C*, 85, 1013, doi: [10.1140/epjc/s10052-025-14720-x](https://doi.org/10.1140/epjc/s10052-025-14720-x)
- Yang, W., Giarè, W., Pan, S., et al. 2023, *Phys. Rev. D*, 107, 063509, doi: [10.1103/PhysRevD.107.063509](https://doi.org/10.1103/PhysRevD.107.063509)
- Yang, W., Pan, S., Di Valentino, E., Mena, O., & Melchiorri, A. 2021, *JCAP*, 10, 008, doi: [10.1088/1475-7516/2021/10/008](https://doi.org/10.1088/1475-7516/2021/10/008)
- Yang, Y., Ren, X., Wang, Q., et al. 2024, *Sci. Bull.*, 69, 2698, doi: [10.1016/j.scib.2024.07.029](https://doi.org/10.1016/j.scib.2024.07.029)
- Yuan, G.-W., Lei, L., Wang, Y.-Z., et al. 2024, *Sci. China Phys. Mech. Astron.*, 67, 109512, doi: [10.1007/s11433-024-2433-3](https://doi.org/10.1007/s11433-024-2433-3)
- Zhang, Y.-M., Li, T.-N., Du, G.-H., et al. 2025. <https://arxiv.org/abs/2510.12627>
- Zhou, S.-H., Li, T.-N., Du, G.-H., et al. 2025, *Phys. Rev. D*, 112, 123532, doi: [10.1103/mtdg-hbqt](https://doi.org/10.1103/mtdg-hbqt)
- Ziegler, J. J., Freese, K., Lozano, J., & Montefalcone, G. 2025. <https://arxiv.org/abs/2507.21409>
- Zuckerman, E., & Anchordoqui, L. A. 2022, *JHEAp*, 33, 10, doi: [10.1016/j.jheap.2021.10.002](https://doi.org/10.1016/j.jheap.2021.10.002)